

Interplay between Gliotoxin Resistance, Secretion, and the Methyl/Methionine Cycle in *Aspergillus fumigatus*

Rebecca A. Owens,^a Grainne O'Keeffe,^a Elizabeth B. Smith,^a Stephen K. Dolan,^a Stephen Hammel,^a Kevin J. Sheridan,^a David A. Fitzpatrick,^a Thomas M. Keane,^b Gary W. Jones,^a Sean Doyle^a

Department of Biology, Maynooth University, Maynooth, Co. Kildare, Ireland^a; The Wellcome Trust Sanger Institute, Hinxton, Cambridge, United Kingdom^b

Mechanistic studies on gliotoxin biosynthesis and self-protection in *Aspergillus fumigatus*, both of which require the gliotoxin oxidoreductase GliT, have revealed a rich landscape of highly novel biochemistries, yet key aspects of this complex molecular architecture remain obscure. Here we show that an *A. fumigatus* $\Delta gliA$ strain is completely deficient in gliotoxin secretion but still retains the ability to efflux bisdethiobis(methylthio)gliotoxin (BmGT). This correlates with a significant increase in sensitivity to exogenous gliotoxin because gliotoxin trapped inside the cell leads to (i) activation of the *gli* cluster, as disabling *gli* cluster activation, via *gliZ* deletion, attenuates the sensitivity of an *A. fumigatus* $\Delta gliT$ strain to gliotoxin, thus implicating cluster activation as a factor in gliotoxin sensitivity, and (ii) increased methylation activity due to excess substrate (dithiol gliotoxin) for the gliotoxin bis-thiomethyltransferase GtmA. Intracellular dithiol gliotoxin is oxidized by GliT and subsequently effluxed by GliA. In the absence of GliA, gliotoxin persists in the cell and is converted to BmGT, with levels significantly higher than those in the wild type. Similarly, in the $\Delta gliT$ strain, gliotoxin oxidation is impeded, and methylation occurs unchecked, leading to significant S-adenosylmethionine (SAM) depletion and S-adenosylhomocysteine (SAH) overproduction. This in turn significantly contributes to the observed hypersensitivity of *gliT*-deficient *A. fumigatus* to gliotoxin. Our observations reveal a key role for GliT in preventing dysregulation of the methyl/methionine cycle to control intracellular SAM and SAH homeostasis during gliotoxin biosynthesis and exposure. Moreover, we reveal attenuated GliT abundance in the *A. fumigatus* $\Delta gliK$ strain, but not the $\Delta gliG$ strain, following exposure to gliotoxin, correlating with relative sensitivities. Overall, we illuminate new systems interactions that have evolved in gliotoxin-producing, compared to gliotoxin-naive, fungi to facilitate their cellular presence.

Biosynthesis, self-protection mechanisms, and functionality of gliotoxin and related epidithiodiketopiperazine (ETP) molecular species, such as chaetocin and acetylaranotin, are attracting ever-increasing attention as a consequence of findings from high-throughput genome sequencing projects, application of gene deletion technologies, and mass spectrometric analytical methodologies (1–5). Indeed, existing paradigms of gliotoxin (Fig. 1) as a toxin and the perspective of the disulfide bridge-containing (oxidized) form as the final, or only, product are undergoing significant reconsideration (6–11).

Self-protection against disulfide-containing metabolites appears to be essential in both fungi and bacteria. It has been demonstrated that the gliotoxin oxidoreductase GliT (12), encoded within the *gli* cluster, protects *Aspergillus fumigatus* against exogenous gliotoxin and is essential for gliotoxin biosynthesis (12, 13). A similar mechanism for self-protection against holomycin in *Streptomyces clavuligerus* has been described, where HlmI catalyzes disulfide bridge closure in holomycin (14). Deletion of *hlmI* impaired holomycin biosynthesis and sensitized *S. clavuligerus* to exogenous holomycin, as had been observed for gliotoxin in *A. fumigatus*. Additionally, Guo et al. revealed that in *Aspergillus terreus*, a fusion gene, *ataTC*, encodes both hydroxylation and disulfide bridge closure of biosynthetic intermediates during acetylaranotin formation (3). Wild-type *A. terreus* did not exhibit acetylaranotin sensitivity; however, no data were presented regarding the sensitivity of the $\Delta ataTC$ strain to exogenous acetylaranotin. Deletion of a major facilitator superfamily (MFS) transporter, *gliA*, and *gliK*, a γ -glutamyl cyclotransferase, also sensitizes *A. fumigatus* to exogenous gliotoxin albeit to a lesser extent than in the absence of GliT (7, 15). While *gliK* deletion prevents gliotoxin biosynthesis (5, 7), interestingly, Wang et al. (15) noted only a

reduction, not an abolition, of gliotoxin secretion by the *A. fumigatus* $\Delta gliA$ strain. Although *gli* cluster gene expression was shown previously to be activated by gliotoxin exposure (13, 16), no evidence of concomitant *de novo* gliotoxin biosynthesis had been detected. However, O'Keeffe et al. (17) demonstrated that *de novo* gliotoxin biosynthesis is induced by the addition of exogenous gliotoxin, which suggests that the significant inhibitory effect of exogenous gliotoxin on the *A. fumigatus* $\Delta gliT$ strain (12, 13) could, in part, also be due to the presence of newly synthesized gliotoxin or a *gli* pathway intermediate. However, surprisingly, the combined impact of the loss of gliotoxin biosynthesis, consequent to *gliZ* deletion, and GliT-mediated self-protection has not been explored to date.

In bacteria, thiomethylation has been posited to be an additional or backup strategy, for disulfide bridge closure, for self-protection during holomycin biosynthesis, and it has been proposed that S-methylation of biosynthetic intermediates, or

Received 18 March 2015 Accepted 30 June 2015

Accepted manuscript posted online 6 July 2015

Citation Owens RA, O'Keeffe G, Smith EB, Dolan SK, Hammel S, Sheridan KJ, Fitzpatrick DA, Keane TM, Jones GW, Doyle S. 2015. Interplay between gliotoxin resistance, secretion, and the methyl/methionine cycle in *Aspergillus fumigatus*. Eukaryot Cell 14:941–957. doi:10.1128/EC.00055-15.

Address correspondence to Gary W. Jones, gary.jones@nuim.ie, or Sean Doyle, sean.doyle@nuim.ie.

Supplemental material for this article may be found at <http://dx.doi.org/10.1128/EC.00055-15>.

Copyright © 2015, American Society for Microbiology. All Rights Reserved. doi:10.1128/EC.00055-15

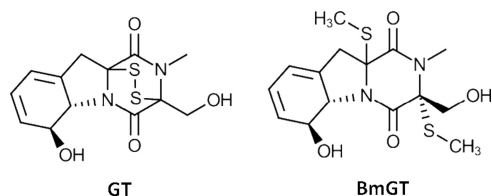


FIG 1 Structures of gliotoxin (GT) and bisdethiobis(methylthio)gliotoxin (BmGT).

possibly shunt metabolites, protects cellular components against these reactive species (14). Moreover, multiple *S*-methylated intermediates have been identified in wild-type *A. fumigatus* but not in an *A. fumigatus* strain deficient in gliotoxin biosynthesis (Δ gliZ) (9). Although bisdethiobis(methylthio)gliotoxin (BmGT) (Fig. 1) has not been reported in most studies relating to *gliT*, *gliA*, *gliK*, or *gliG* (a glutathione *S*-transferase responsible for biosynthetic intermediate sulfurization via *bis*-glutathionylation) gene cluster deletion (4, 5, 7, 13, 15, 18, 19), this metabolite is readily detectable in culture supernatants of *A. fumigatus* (8–10). Moreover, endogenous dithiol gliotoxin [GT-(SH)₂] and exogenous gliotoxin can be converted to BmGT via a novel, *S*-adenosylmethionine (SAM)-dependent gliotoxin *bis*-thiomethyltransferase (GtmA) (10). Contrary to speculation in the literature (14) that deficiency of such an enzyme would induce gliotoxin sensitivity in *A. fumigatus*, as per deletion of *gliT*, no such phenotype has been observed. Indeed, *gtmA* deletion leads to the overproduction of gliotoxin, which positions BmGT formation as a negative regulatory mechanism of gliotoxin biosynthesis (10). However, the effects of gliotoxin *bis*-thiomethylation on the methionine cycle and cellular SAM and *S*-adenosylhomocysteine (SAH) levels in *A. fumigatus* remain obscure.

SAM is also involved in gliotoxin biosynthesis, where it provides a methyl group for *N*-methylation of the diketopiperazine scaffold during biosynthesis (4, 20, 21). Moreover, if *S*-methylation is involved in the modification of reactive biosynthetic intermediates, or shunt metabolites (9), SAM may also be the source of these methyl groups. SAM is derived from methionine, and while much work has been done on methionine biosynthesis in *Aspergillus nidulans*, until recently (22), few studies had specifically focused on sulfur metabolism in *A. fumigatus*. Moreover, there appears to be a dearth of literature pertaining to the functionality and detection of SAM in *A. fumigatus*. Enzyme-catalyzed *S*-methylation reactions using SAM yield SAH, which in *A. nidulans* and other organisms is subsequently hydrolyzed to homocysteine (Hcy) and adenosine via the action of *S*-adenosylhomocysteinase. The resultant Hcy is then reconverted to Met via the action of methionine synthase, with methylenetetrahydrofolate (from the methyl cycle) as the methyl source (23, 24). Notably, SAH is a competitive inhibitor of selected methyltransferases, and Hcy is cytotoxic, in *A. nidulans* (25, 26). These enzyme systems have received scant attention in *A. fumigatus*, which is of major significance because of the potential interplay between gliotoxin biosynthesis, SAM availability, and *bis*-thiomethylation, especially in the absence of *gliT*. Moreover, in the absence of gliotoxin biosynthesis in *A. nidulans*, the nature of the systems interactions between primary and so-called secondary metabolisms is refractory to investigation. The work presented here describes how gliotoxin biosynthesis, resistance, and secretion may be integrated

into primary metabolism via *bis*-thiomethylation and SAM:SAH homeostasis. Furthermore, we reveal a key role for *GliT* in preventing dysregulation of SAM:SAH homeostasis.

MATERIALS AND METHODS

Gene deletion, complementation, and gene expression analyses of *A. fumigatus*. *A. fumigatus* Δ gliA and Δ gliZ:: Δ gliT strains were generated via the bipartite marker technique, using either the pyrithiamine resistance gene (*ptrA*) (Δ gliA and Δ gliZ:: Δ gliT) or the hygromycin resistance gene (*hph*) (*gliA* complemented [*gliA*^C] and Δ gliZ:: Δ gliT::*gliZ*) for selection (27–29). All strains used are given in Table S1 in the supplemental material. Primers used for generating deletion constructs are given in Table S2 in the supplemental material. The Δ gliZ:: Δ gliT double mutant and the Δ gliZ:: Δ gliT::*gliZ* complemented strain were generated in the background of the *A. fumigatus* Δ gliZ strain, kindly provided by Nancy Keller (University of Wisconsin—Madison). The *A. fumigatus* Δ metR strain was generously provided by Sven Krappmann (Erlangen, Germany). Fungal RNA isolation, DNase treatment, cDNA synthesis, and reverse transcription-quantitative PCR (qRT-PCR) were performed as described previously (30). Primers used for qRT-PCRs are listed in Table S2 in the supplemental material. qRT-PCR analysis was performed by using a Roche Light Cycler 480 instrument.

LC-MS detection of gliotoxin and BmGT. *A. fumigatus* wild-type, Δ gliA, and *gliA*^C cultures were either grown for 72 to 96 h in Czapek Dox medium, to examine endogenous gliotoxin/BmGT production, or for 21 h in Czapek Dox medium followed by a 3-h challenge with gliotoxin (5- μ g/ml final concentration), to examine the conversion of exogenous gliotoxin to BmGT. BmGT formation in the *A. fumigatus* Δ gliT strain was identically evaluated. Culture supernatants were subjected to organic extraction and liquid chromatography-mass spectrometry (LC-MS) analysis to detect gliotoxin and BmGT, as previously described (7, 10). GtmA activity in the *A. fumigatus* Δ gliK strain was determined as described previously for the *A. fumigatus* Δ gliT strain (10). Statistical analyses were carried out by using Student's *t* test.

Detection and quantification of *S*-adenosylmethionine and *S*-adenosylhomocysteine. Czapek Dox medium was inoculated with 10⁶ conidia/ml (from *A. fumigatus* wild-type, gene deletion, and complementation strains), in duplicate, and incubated at 37°C, with shaking 200 rpm, for 21 h. Gliotoxin (5- μ g/ml final concentration) or the methanol control was added, and the cultures were incubated for a further 3 h before mycelia were harvested and snap-frozen in liquid N₂. SAM and SAH were extracted according to a modified protocol (31, 32). Briefly, mycelia were ground under liquid N₂ by using a pestle and mortar. A total of 0.1 M HCl (250 μ l) was added to mycelia (100 mg), and the mixture was incubated on ice for 1 h with regular vortexing. Following centrifugation at 13,000 \times g, protein was removed from the supernatant by trichloroacetic acid (TCA) precipitation. Samples were diluted in 0.1% (vol/vol) formic acid and analyzed by LC-tandem MS (MS/MS) using a porous graphitized carbon (PGC) chip on an Agilent 6340 Ion-Trap LC mass spectrometer (Agilent Technologies), using electrospray ionization. Quantification was enabled by using commercially available SAM and SAH obtained from Sigma-Aldrich. Intracellular gliotoxin and BmGT in wild-type and *A. fumigatus* Δ gliA strains were analyzed by using a C₁₈ chip, and analysis of gliotoxin biosynthetic intermediates in the *A. fumigatus* Δ gliK strain, via PGC chip analysis, was also facilitated by using this extraction procedure. Statistical analyses were carried out by using Student's *t* test.

***A. fumigatus* whole-protein extraction for 2D-PAGE, LC-MS, and protein identification.** Comparative two-dimensional PAGE (2D-PAGE) analysis of the *A. fumigatus* Δ gliK strain following exposure to gliotoxin was carried out to investigate gross proteome changes associated with gliotoxin sensitivity. The *A. fumigatus* Δ gliK strain was cultured in Sabouraud dextrose medium for 24 h before the addition of gliotoxin (10- μ g/ml final concentration) or the equivalent volume of methanol as a

control ($n = 5$ biological replicates). After 4 h, mycelia were harvested, and protein was extracted. Harvested mycelia were prepared for 2D-PAGE, protein spots were digested with trypsin, and LC-MS analysis (Agilent) was performed essentially as described previously (11, 29, 33).

Label-free quantitative proteomic analysis of *A. fumigatus* wild-type Δ gliK, Δ gliK, and Δ gliG strains. *A. fumigatus* ATCC 26933, Af293, ATCC 26933 Δ gliK mutant (Δ gliK^{ATCC 26933}), and Δ gliG^{Af293} mutant strains were cultured in Sabouraud dextrose medium for 21 h, followed by the addition of gliotoxin (5- μ g/ml final concentration) or methanol for 3 h ($n = 3$ to 4 biological replicates for all specimens). Comparative label-free quantitative (LFQ) proteomic analysis of *A. fumigatus* ATCC 26933 versus the *A. fumigatus* Δ gliA^{ATCC 26933} strain was performed following culture in Czapek Dox medium for 72 h ($n = 3$ biological replicates). Mycelial lysates were prepared in lysis buffer (100 mM Tris-HCl, 50 mM NaCl, 20 mM EDTA, 10% [vol/vol] glycerol, 1 mM phenylmethylsulfonyl fluoride [PMSF], 1 μ g/ml pepstatin A [pH 7.5]) with grinding and sonication and were clarified by centrifugation. The resultant protein lysates were precipitated by using TCA-acetone and resuspended in 8 M urea. After dithiothreitol (DTT) reduction and iodoacetamide-mediated alkylation (11, 33), sequencing-grade trypsin combined with ProteaseMax surfactant was added. Digested samples were desalted prior to analysis by using either C₁₈ spin columns (Thermo Scientific Pierce) or C₁₈ ZipTips (Millipore). All peptide mixtures were analyzed via a Thermo Scientific Q-Exactive mass spectrometer coupled to a Dionex RSLCnano instrument. LC gradients from 4 to 35% or 10 to 35% solution B (solution A is 0.1% [vol/vol] formic acid, and solution B is 80% [vol/vol] acetonitrile plus 0.1% [vol/vol] formic acid) were run over 2 h, and data were collected by using the Top15 method for MS/MS scans. Comparative proteome abundance and data analyses were performed by using MaxQuant software (version 1.3.0.5) (34), with Andromeda being used for database searching and Perseus (version 1.4.1.3) being used to organize the data. Carbamidomethylation of cysteines was set as a fixed modification, while oxidation of methionine and acetylation of N termini were set as variable modifications. The maximum peptide/protein false discovery rates (FDRs) were set to 1% based on comparison to a reverse database. The LFQ algorithm was used to generate normalized spectral intensities and infer relative protein abundance. Proteins that matched to a contaminant database or the reverse database were removed, and proteins were retained for final analysis only if they were detected in at least three replicates from at least one sample. Quantitative analysis was performed by using a *t* test to compare pairs of samples, and proteins with significant changes in abundance (P value of <0.05 ; fold change of ≥ 2) were included in the quantitative results. Qualitative analysis was also performed to detect proteins that were found in at least 3 replicates for a particular sample but undetectable in the comparison sample. Gene Ontology (GO) term enrichment ($P < 0.05$) was investigated by using the FungiFun application (35). All subsets of proteins were compared to a background consisting of the total identified proteins from the respective studies.

Phenotypic assays. Conidia (10^6), harvested aseptically from 1-week-old *Aspergillus* minimal medium (AMM) plates, were subject to a variety of phenotypic assays. Plates were incubated at 37°C. Colony diameters were measured periodically, and statistical analysis was carried out by using one-way analysis of variance (ANOVA).

RESULTS

Absence of GliA abolishes gliotoxin, but not BmGT, secretion. Deletion, complementation, and expression of *A. fumigatus* *gliA*, an MFS transporter proposed to be partly responsible for gliotoxin secretion (15), were confirmed by Southern blotting, PCR, and RT-PCR/qRT-PCR (see Fig. S1 in the supplemental material). Unexpectedly, the absence of *gliA* completely and specifically abolished the secretion of endogenous gliotoxin (Fig. 2A), yet BmGT was secreted by the *A. fumigatus* Δ gliA strain at significantly higher levels than those in the wild type ($P < 0.0001$) at 72 h (Fig. 2A, inset). Complementation of *gliA* in the *A. fumigatus*

Δ gliA strain (see Fig. S1 in the supplemental material) restored gliotoxin secretion (Fig. 2A). Following exposure to exogenous gliotoxin in liquid culture, BmGT was produced by the *A. fumigatus* Δ gliA strain at significantly higher levels than those in the wild type at both 15 min ($P = 0.005$) and 30 min ($P = 0.002$), yet the Δ gliA strain was significantly sensitive ($P < 0.0001$) to exogenous gliotoxin (5 μ g/ml) (Fig. 2B and C) albeit to a lesser extent than the *A. fumigatus* Δ gliT strain. This observation suggests that gliotoxin bis-thiomethylation is not primarily involved in, or sufficient for, protection against the growth-inhibitory effects of gliotoxin, in the absence of the ability to secrete gliotoxin.

Intracellular gliotoxin and significantly elevated levels of intracellular BmGT were detectable in the *A. fumigatus* Δ gliA strain due to its inability to efflux gliotoxin, which results in significantly elevated expression levels of both the *gli* cluster (positive-feedback) (16) and *gtmA* (negative-feedback) (10) systems (Fig. 2D). Consequently, at between 48 and 96 h, this resulted in a significantly higher level of BmGT efflux in the *A. fumigatus* Δ gliA strain. Accordingly, although exogenous gliotoxin was not detected, Fig. 2E shows that the *gtmA* (10) expression level was significantly elevated ($P = 0.0392$) in the *A. fumigatus* Δ gliA strain at 72 h, as was the *gliT* expression level ($P = 0.0060$) (see Fig. S1 in the supplemental material), under conditions permissive for gliotoxin biosynthesis, which suggests cross talk between intracellular gliotoxin and *gtmA* expression. It is also notable that *gtmA* expression was restored to wild-type levels in the *A. fumigatus* *gliA*^C strain (Fig. 2E).

gliA deletion alters the *A. fumigatus* proteome. Label-free quantitative (LFQ) proteomic investigation of wild-type *A. fumigatus* versus the Δ gliA strain further underpinned the impact of the accrual of intracellular gliotoxin on *gliA* deletion. Compared to the wild type, the abundances of 92 proteins were significantly increased in the *A. fumigatus* Δ gliA strain, including GtmA ($P < 0.00015$), GliT ($P < 0.01097$), GliM ($P < 0.00703$), and GliN ($P < 0.02596$) (Table 1). To our knowledge, this is the first demonstration that disruption of the secretion of endogenous gliotoxin induces altered abundances of gliotoxin and BmGT biosynthetic enzymes in *A. fumigatus*. Moreover, this finding is entirely confluent with observations of increased *gtmA* (Fig. 2E) and *gliT* (see Fig. S1 in the supplemental material) (15) expression levels and significantly increased intracellular BmGT formation, as described above. Additionally, analysis of GO term enrichment revealed significant increases in the abundances of proteins involved in protein modification (3 proteins; $P = 0.01312$) and fatty acid biosynthetic processes (2 proteins; $P = 0.0250$) in the Δ gliA strain compared to the wild type. Proteins found in lower abundances in the Δ gliA strain than in the wild type were significantly enriched for translation (2 proteins; $P = 0.0006$), tRNA modification (2 proteins; $P = 0.0087$), and lipid metabolic processes (3 proteins; $P = 0.0315$). Methylation was significantly enriched among proteins with both increased (6 proteins; $P = 0.00118$) and decreased (7 proteins; $P = 0.0145$) abundances in the Δ gliA strain compared to the wild type.

Attenuated sensitivity to gliotoxin in the *A. fumigatus* Δ gliZ:: Δ gliT strain and BmGT overproduction in the *A. fumigatus* Δ gliT strain. In order to evaluate the impact of a combined deficit in gliotoxin biosynthesis and self-protection against exogenous gliotoxin, an *A. fumigatus* Δ gliZ:: Δ gliT double mutant was generated in a Δ gliZ background. As shown in Fig. S1 in the supplemental material, *gliT* loss in the *A. fumigatus* Δ gliZ strain

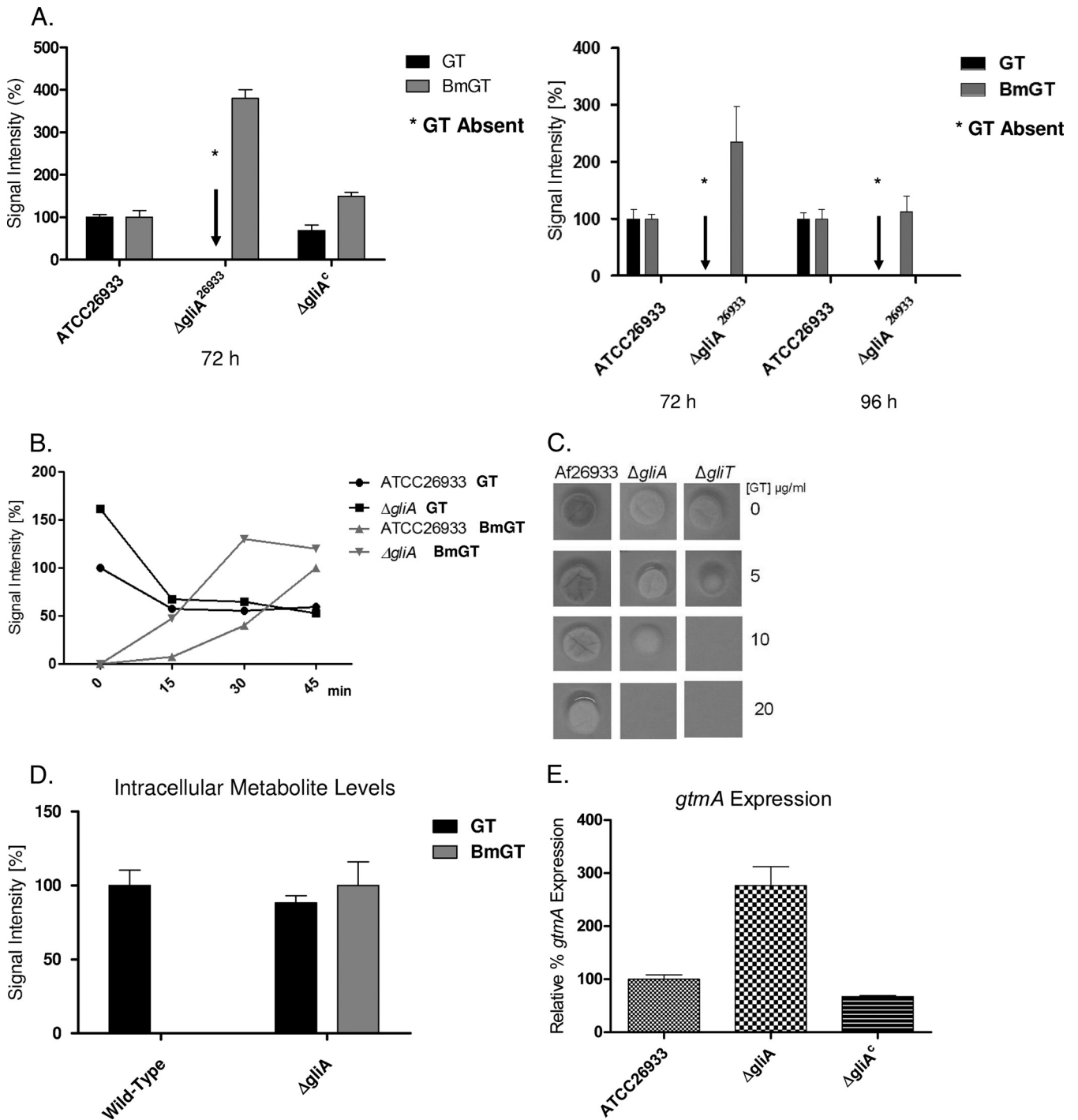


FIG 2 Characterization of the *A. fumigatus* $\Delta gliA$ strain. (A) Deletion of *gliA* completely abrogates gliotoxin, but not BmGT, secretion. *gliA* complementation restores gliotoxin secretion. The inset shows that *gliA* deletion also results in significantly increased BmGT secretion ($P < 0.0001$) at 72 h but not at 96 h of culture. (B) Exogenously added gliotoxin is converted to BmGT, and secreted, at a significantly higher rate in the *A. fumigatus* $\Delta gliA$ strain than in the wild type up to 30 min postaddition. (C) The *A. fumigatus* $\Delta gliA$ strain exhibits increased sensitivity to exogenous gliotoxin compared to the wild type. However, the *A. fumigatus* $\Delta gliA$ strain is not as sensitive to exogenous gliotoxin as the *A. fumigatus* $\Delta gliT$ strain (13). (D) Deletion of *gliA* results in accumulation of intracellular BmGT. (E) Comparative qRT-PCR analysis of *gtmA* expression in *A. fumigatus* wild-type, $\Delta gliA$, and $\Delta gliA^c$ strains at 72 h. Significantly elevated *gtmA* expression levels are evident in the $\Delta gliA$ strain compared to those in the wild-type ($P = 0.0392$) and $\Delta gliA^c$ ($P = 0.0272$) strains. Statistical analysis was performed by using Student's *t* test.

TABLE 1 LFQ proteomics analysis of proteins with increased abundance in, or that are unique to, the *A. fumigatus* $\Delta gliA^{ATCC 26933}$ strain compared to wild-type *Aspergillus fumigatus* strain ATCC 26933^a

Protein description	Log ₂ -fold increase	P value	No. of peptides	Sequence coverage (%)	CADRE identification no.
Gamma-glutamyltranspeptidase	Unique	NA	4	13.3	AFUA_4G13580
Conserved hypothetical protein	Unique	NA	3	15.3	AFUA_5G02820
Putative isopenicillin N-CoA epimerase; transcript upregulated in conidia exposed to neutrophils	Unique	NA	2	8.9	AFUA_5G03740
Protein with ortholog(s) that has plasma membrane localization	Unique	NA	4	28.3	AFUA_5G06540
Protein with ortholog(s) that has a role in cytoplasmic translation, and cell tip and cytoplasm localization	Unique	NA	4	13	AFUA_5G06770
Protein with ortholog(s) that has mitochondrial ribosome localization	Unique	NA	3	9.4	AFUA_5G09500
Protein with ortholog(s) that has an Elg1 RFC-like complex and cytosol and nucleus localization	Unique	NA	3	15.2	AFUA_6G05040
Protein of unknown function; calcium downregulated	Unique	NA	2	7.5	AFUA_6G14280
Putative 14- α demethylase with a predicted role in ergosterol biosynthesis; transcript upregulated in response to amphotericin B; SrbA regulated during hypoxia	Unique	NA	2	5.3	AFUA_7G03740
Hypothetical protein	Unique	NA	5	15	AFUA_3G02430
Putative pyridoxamine phosphate oxidase; transcript upregulated in conidia exposed to neutrophils	Unique	NA	2	11.9	AFUA_3G06670
Putative aryl-alcohol dehydrogenase	Unique	NA	9	31.4	AFUA_4G00610
Sterol 24- <i>c</i> -methyltransferase, putative	Unique	NA	6	29.2	AFUA_4G03630
Protein with ortholog(s) that has DNA binding and tricarboxylate secondary active transmembrane transporter activity and roles in alpha-ketoglutarate transport, mitochondrial citrate transport, and mitochondrial genome maintenance	Unique	NA	4	20.8	AFUA_5G04220
Conserved hypothetical protein	Unique	NA	2	25.6	AFUA_5G04336
DUF453 domain protein	Unique	NA	2	10.7	AFUA_6G00360
GliF	Unique	NA	5	14.3	AFUA_6G09730
Putative cyclophilin; peptidyl-prolyl <i>cis-trans</i> -isomerase	Unique	NA	3	21.6	AFUA_6G10480
Predicted aminopeptidase, metalloexopeptidase; encoded in the <i>fma</i> (fumagillin) secondary metabolite gene cluster	Unique	NA	3	17.4	AFUA_8G00460
GtmA	2.26265	0.00015	11	53.4	AFUA_2G11120
GliM	2.08787	0.00703	17	65.4	AFUA_6G09680
GliT thioredoxin reductase	1.52564	0.01097	15	80.2	AFUA_6G09740
GliN	1.37247	0.02596	12	58.2	AFUA_6G09720

^a Data are sorted by fold change, in descending order. Statistical analysis was performed by using Student's *t* test. NA, not applicable; CoA, coenzyme A; RFC, replication factor C.

was confirmed, whereby a 3.64-kb fragment was evident in both the double mutant and the *A. fumigatus* $\Delta gliT^{ATCC 26933}$ strain (positive control) (13). While the *A. fumigatus* $\Delta gliZ::\Delta gliT$ strain displayed mild sensitivity to exogenous gliotoxin (5 μ g/ml), unexpectedly, this sensitivity was significantly lower ($P = 0.0131$) than that observed for the *A. fumigatus* $\Delta gliT$ strain ($P = 0.0028$) (Fig. 3A); thus, *gli* cluster expression and endogenous gliotoxin formation appear to be essential for the manifestation of gliotoxin sensitivity of the *A. fumigatus* $\Delta gliT$ strain. Exposure of the *A. fumigatus* $\Delta gliT$ strain to gliotoxin resulted in significantly increased production and secretion ($P = 0.0039$) of BmGT compared to wild-type exposure (Fig. 3B). Since SAM is required for BmGT biosynthesis, if this observation was accompanied by dysregulation of SAM:SAH homeostasis, then an important link between so-called primary and secondary metabolisms may be revealed.

Exposure of *A. fumigatus* to gliotoxin depletes SAM and augments SAH levels in the absence of *gliT*. Exogenous gliotoxin had no significant impact on the levels of SAM and SAH in *A. fumigatus* ATCC 46645 (low-gliotoxin producer), while in ATCC 26933 (high-gliotoxin producer), there was no alteration in SAM levels,

but there was a significant increase ($P = 0.0157$) in SAH levels (Fig. 4A and B). No significant difference in cellular SAM and SAH levels was noted following exposure of *A. fumigatus* Af293 (36) to exogenous gliotoxin under conditions permissive for gliotoxin biosynthesis (Fig. 4C). The response of the *A. fumigatus* $\Delta gliG$ strain to gliotoxin exposure is equivalent to that of the background strain (Af293) (Fig. 4C), especially with respect to the maintenance of SAM levels. Under conditions that promote gliotoxin biosynthesis (7), gliotoxin exposure induced the depletion and production of SAM and SAH, respectively, in the *A. fumigatus* $\Delta gliT$, $\Delta gliK$, $\Delta gliZ$, and $\Delta gliZ::\Delta gliT$ strains (Fig. 4A to C). The altered SAM:SAH homeostasis in the $\Delta gliK$ strain is interesting, as this strain is sensitive to exogenous gliotoxin. Indeed, it is clear that cellular SAH levels are most significantly increased in the $\Delta gliT^{ATCC 46645}$ and $\Delta gliT^{ATCC 26933}$ strains ($P = 0.0135$ and $P = 0.0002$, respectively), with significant depletion of SAM levels in the $\Delta gliT^{ATCC 46645}$ strain ($P = 0.0359$) and the $\Delta gliT^{ATCC 26933}$ strain ($P = 0.0028$) (Fig. 4A and B), the *gli* single-deletion strain whose growth is most inhibited by exogenous gliotoxin, compared to all other strains tested. *gliT* complementation restores the wild-type scenario (Fig. 4A and B). Indeed, the deletion of *gliT* in

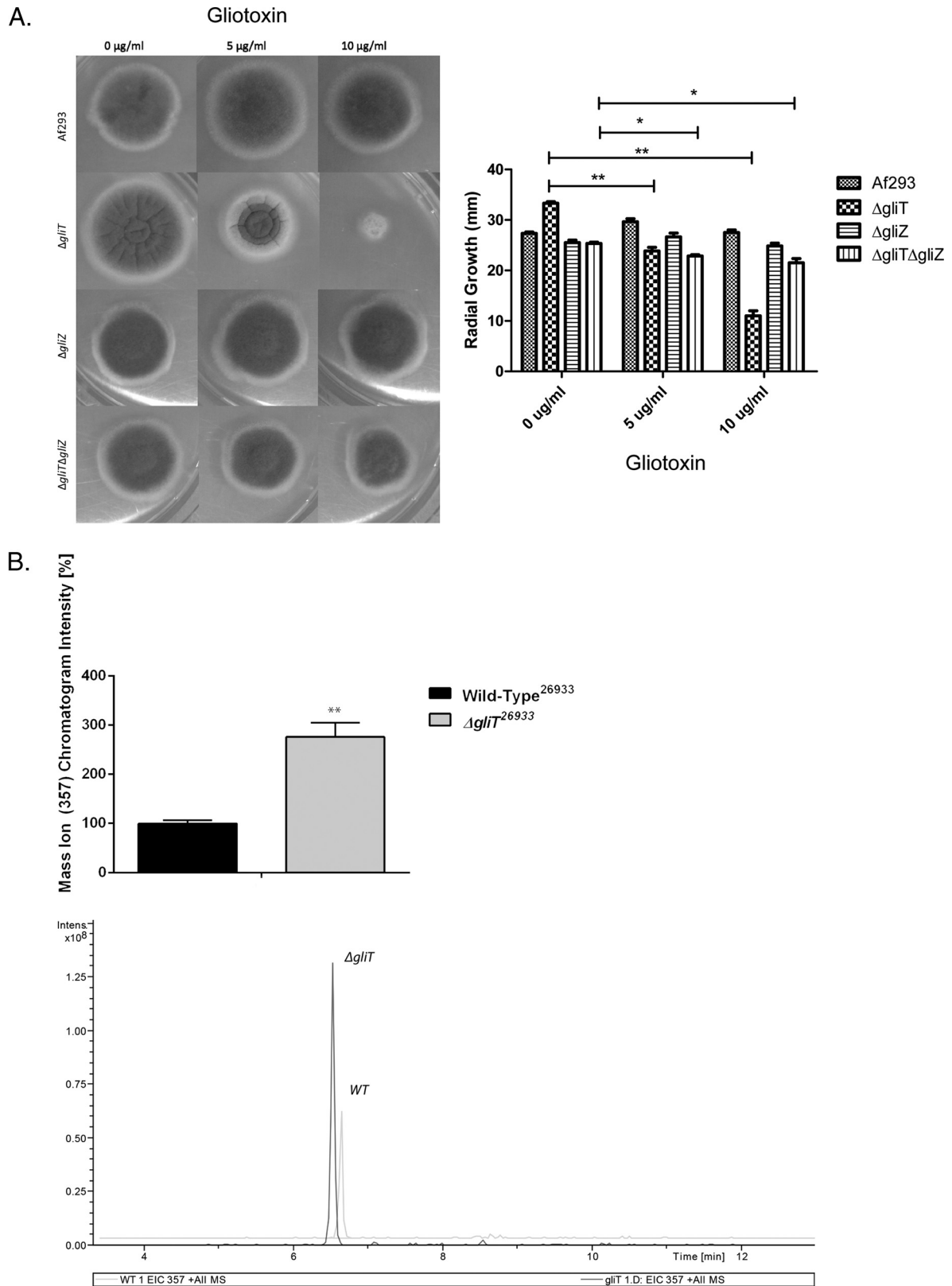


FIG 3 Evaluation of the effect of a combined deficit in biosynthesis and self-protection on *A. fumigatus* sensitivity to exogenous gliotoxin. (A) The *A. fumigatus* $\Delta\text{gliZ}::\Delta\text{gliT}$ strain, deficient in both gliotoxin biosynthesis and self-protection systems, is significantly less sensitive ($P = 0.0237$) to exogenous gliotoxin than the *A. fumigatus* ΔgliT strain ($P = 0.0011$). (B) LC-MS analysis reveals significantly elevated BmGT secretion by the *A. fumigatus* ΔgliT compared to wild-type *A. fumigatus* when exposed to exogenous gliotoxin (5 $\mu\text{g/ml}$ for 3 h; $n = 3$). The inset shows results for BmGT detection in the *A. fumigatus* ΔgliT strain following gliotoxin exposure by LC-MS. EIC, extracted ion chromatograph.

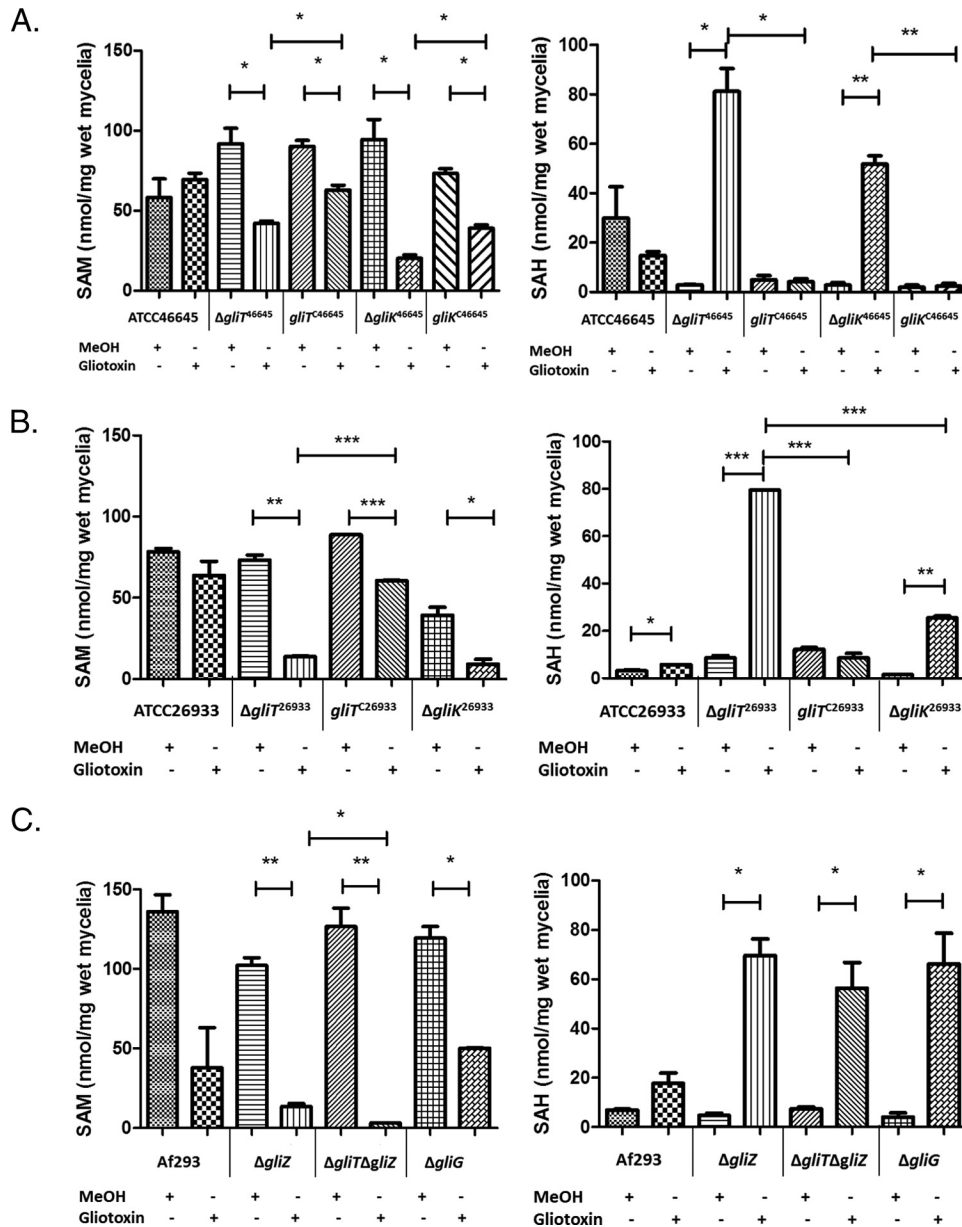


FIG 4 Quantitative determination of cellular SAM and SAH levels in *A. fumigatus* mycelial extracts by LC-MS analysis. (A) Effect of gliotoxin exposure (5 μ g/ml for 3 h) on SAM and SAH levels in *A. fumigatus* ATCC 46645 and the $\Delta gliT^{ATCC 46645}$, $\Delta gliT^{CATCC 46645}$, $\Delta gliK^{ATCC 46645}$, and $\Delta gliK^{CATCC 46645}$ mutants. (B) Effect of gliotoxin exposure (5 μ g/ml for 3 h) on SAM and SAH levels in *A. fumigatus* ATCC 26933 and the $\Delta gliT^{ATCC 26933}$, $gliT^{CATCC 26933}$, and $\Delta gliK^{ATCC 26933}$ mutants. Compared to the wild-type and complemented strains, gliotoxin exposure results in significant or highly significant SAM depletion and SAH production in both the $\Delta gliK$ and $\Delta gliT$ strains, irrespective of the strain background. The level of SAH production is also significantly higher in the $\Delta gliT^{ATCC 26933}$ strain than in the $\Delta gliK^{ATCC 26933}$ strain. (C) Effect of gliotoxin exposure (5 μ g/ml for 3 h) on SAM and SAH levels in *A. fumigatus* Af293 and the $\Delta gliZ$, $\Delta gliZ::\Delta gliT$, and $\Delta gliG^{A293}$ mutants. SAM depletion in the *A. fumigatus* $\Delta gliZ::\Delta gliT$ strain is significantly enhanced compared to that in the *A. fumigatus* $\Delta gliZ$ strain. Although significantly depleted by the addition of gliotoxin, the absolute SAM level in the $\Delta gliG$ strain is higher than those in all other deletion mutants. *, $P < 0.05$; **, $P < 0.01$; ***, $P < 0.001$. Statistical analysis was performed by using Student's *t* test. MeOH, methanol.

the $\Delta gliZ$ strain resulted in further significant cellular SAM depletion compared to that in the $\Delta gliZ$ strain ($P = 0.0377$) upon exogenous gliotoxin exposure (Fig. 4C). We conclude that normal cellular SAM:SAH homeostasis requires GliT to preferentially oxidize GT-(SH)₂ to gliotoxin, thereby preventing GtmA-mediated dysregulation of cellular SAM:SAH homeostasis. In the absence of GliT, it appears that increased SAM-dependent, GtmA-mediated *bis*-thiomethylation of GT-(SH)₂ (10) rapidly depletes SAM and

may result in dysregulation of the methyl/methionine cycle in *A. fumigatus*. Indeed, SAM depletion may also have further implications for global methylation reactions in *A. fumigatus*, and transcriptomic analysis of the $\Delta gliT$ strain exposed to exogenous gliotoxin revealed altered expression levels of a number of methyltransferases (17). Moreover, since GliG activity precedes GliK activity in the gliotoxin biosynthetic pathway, yet the respective deletion strains exhibit resistance or sensitivity to exoge-

nous gliotoxin, respectively, we hypothesized that comparative proteomic analysis may allow dissection of these contrasting phenotypes.

Gliotoxin exposure upregulates the expression of genes involved in sulfur metabolism in the *A. fumigatus* Δ *gliT* strain. Transcriptome sequencing (RNA-seq) analysis (17) revealed that exposure of the *A. fumigatus* Δ *gliT*^{ATCC 46645} strain to gliotoxin resulted in significantly upregulated expression (P value of $<5 \times 10^{-5}$ to 0.005) of genes involved in sulfur assimilation and methionine and SAM biosynthesis (see Table S3 in the supplemental material). Specifically, the expression levels of phosphoadenylyl-sulfate reductase and sulfite reductase were upregulated 3.02 log₂- and 2.55 log₂-fold, respectively, while those of methylenetetrahydrofolate reductase (MTHFR) (*mtrA*), cobalamin-independent methionine synthase (*metH*), and *S*-adenosylmethionine synthetase (*sasA*) were also significantly increased (P value of $<5 \times 10^{-5}$ to 0.003) (see Table S3 in the supplemental material). Expressions of the bZIP transcription factor *metR* (22) and *S*-adenosylhomocysteinase (*sahA*) were also upregulated (P value of <0.00015 to 0.001), as were those of glycine dehydrogenase (GDH) ($P < 0.0056$) and serine hydroxymethyltransferase (SHMT) ($P < 0.0001$) (see Table S3 in the supplemental material). GDH and SHMT act in concert with the folate cycle to transfer methyl groups to Hcy for methionine biosynthesis (37). Interestingly, the *A. fumigatus* Δ *metR* strain showed significantly increased sensitivity to gliotoxin ($P < 0.05$) compared to the wild type (ATCC 46645) (see Fig. S2 in the supplemental material), and qRT-PCR analysis revealed significantly attenuated *gliT* expression ($P < 0.001$) in response to gliotoxin exposure (see Fig. S2 in the supplemental material). Although the Hcy precursor cystathionine (0.5 to 1.5 mM) alone had no effect on the *A. fumigatus* Δ *metR* strain (data not shown), coexposure with gliotoxin (10 μ g/ml) resulted in a significant retardation of growth (1.5 mM cystathionine) ($P < 0.01$) at 72 h compared to that of ATCC 46645 (see Fig. S2 in the supplemental material), which suggests that impaired *gliT* expression may facilitate cystathionine and gliotoxin to interact to cause growth retardation. Overall, these observations reveal the impact of gliotoxin on, and the importance of GliT for, the control of sulfur metabolism. Moreover, these results underpin our observations regarding dysregulated SAM:SAH levels and strongly imply that gliotoxin exposure has an impact on the methyl/methionine cycle of *A. fumigatus* in the absence of *gliT*. This suggests enzyme functionality beyond gliotoxin biosynthesis. To explore this phenomenon further, proteomic approaches were adopted to ascertain the interplay between gliotoxin biosynthesis, resistance, and primary metabolism.

2D-PAGE and label-free quantitative proteomic investigations reveal that exogenous gliotoxin induces proteome remodeling in the *A. fumigatus* Δ *gliK* strain. Following 2D-PAGE, 33 protein spots displayed significant changes in abundance in the *A. fumigatus* Δ *gliK*^{ATCC 26933} strain (19 with ≥ 1.5 -fold-increased and 14 with ≥ 1.5 -fold-decreased abundances; $P < 0.05$) (7) upon exposure to gliotoxin (10 μ g/ml) for 4 h (Fig. 5A and B and Table 2). LC-MS/MS analysis yielded identifications for 31 of these spots, corresponding to 30 distinct proteins. Overall, increased abundances of 18 protein spots, corresponding to 17 distinct *A. fumigatus* proteins, were observed for the Δ *gliK* strain in response to gliotoxin (Table 2). Proteins undergoing significant changes in abundance in the *A. fumigatus* Δ *gliK* strain following exposure to gliotoxin include those involved in translation and amino acid

metabolism, those exhibiting regulatory roles, and endoplasmic reticulum (ER)-associated proteins (Table 2). However, of special significance, the abundance of the cobalamin-independent methionine synthase MetH/D (AFUA_4G07360) was significantly increased (1.9- to 2.2-fold), and that of MTHFR/MtrA was significantly increased (1.8-fold), in response to gliotoxin exposure. Both of these enzymes are essential for methionine biosynthesis (37, 38) and for the operation of the methyl/methionine cycle, which affects SAM biosynthesis.

Interestingly, an increased abundance of the gliotoxin oxidoreductase GliT was not detectable by comparative 2D-PAGE analysis of the *A. fumigatus* Δ *gliK* strain in the presence of gliotoxin, although significantly elevated *gliT* expression levels under near-identical conditions were reported previously (7). This putative sensitivity limitation of 2D-PAGE led us to explore altered protein abundance in the *A. fumigatus* Δ *gliK* strain following gliotoxin exposure by a more sensitive approach, LFQ proteomics. These data reveal that gliotoxin (5 μ g/ml for 3 h) significantly increases the abundance of GliT (log₂ fold change = 3.837; $P = 3.39 \times 10^{-2}$), as well as effecting *de novo* expression of GtmA (10), in the *A. fumigatus* Δ *gliK* strain (Table 3). These findings are in complete accordance with the detection of GtmA activity in gliotoxin induced *A. fumigatus* Δ *gliK* mycelial lysates (Fig. 5C). Importantly, GliT abundance was increased significantly more (log₂ fold change = 7.97; $P = 1.35 \times 10^{-5}$) following exposure of wild-type *A. fumigatus* to gliotoxin under identical conditions (see Table S4 in the supplemental material). In effect, the *A. fumigatus* Δ *gliK* strain is a “GliT-lite” mutant. Moreover, this observation supports the hypothesis of the requirement for *de novo* gliotoxin biosynthesis to effect maximum gliotoxin-mediated growth inhibition, as significantly less GliT is required for GT-(SH)₂ oxidation to gliotoxin in the *A. fumigatus* Δ *gliK* strain, which is itself deficient in gliotoxin biosynthesis and accumulates a *bis*-glutathionylated gliotoxin biosynthetic intermediate at *m/z* 845.3 ([M + H]⁺) (Fig. 5D) (5). Finally, we show that AFUA_5G08600, a putative homoserine *O*-acetyltransferase that provides an alternative route for cystathionine (39) and, ultimately, Hcy biosynthesis, is uniquely expressed in the *A. fumigatus* Δ *gliK* strain following exposure to gliotoxin (Table 3). This may provide an alternative route for SAM formation and provides insight into the integrated nature of gliotoxin resistance/biosynthesis in primary cellular metabolism in *A. fumigatus*.

The GliT-mediated self-protection system is operable in the *A. fumigatus* Δ *gliG* strain. The *A. fumigatus* Δ *gliG* strain is incapable of gliotoxin biosynthesis, and growth is unaffected by the presence of gliotoxin (4). Consequently, this scenario represents an ideal model to further dissect the impact of gliotoxin on *A. fumigatus* metabolic systems. FunCat analysis of the proteins with increased abundances in the *A. fumigatus* Δ *gliG* strain following exogenous gliotoxin exposure revealed enrichment for proteins involved in the oxidative stress response. In addition to other FunCat categories, proteins involved in metabolism of peptide-derived compounds and RNA transport were also significantly represented among proteins with increased abundance upon exogenous gliotoxin exposure in the *A. fumigatus* Δ *gliG* strain. A number of proteins involved in RNA processing and RNA modification, along with some participating in DNA synthesis and replication, were significantly enriched for proteins with decreased abundance in the *A. fumigatus* Δ *gliG* strain exposed to exogenous gliotoxin. Other FunCat categories significantly enriched for pro-

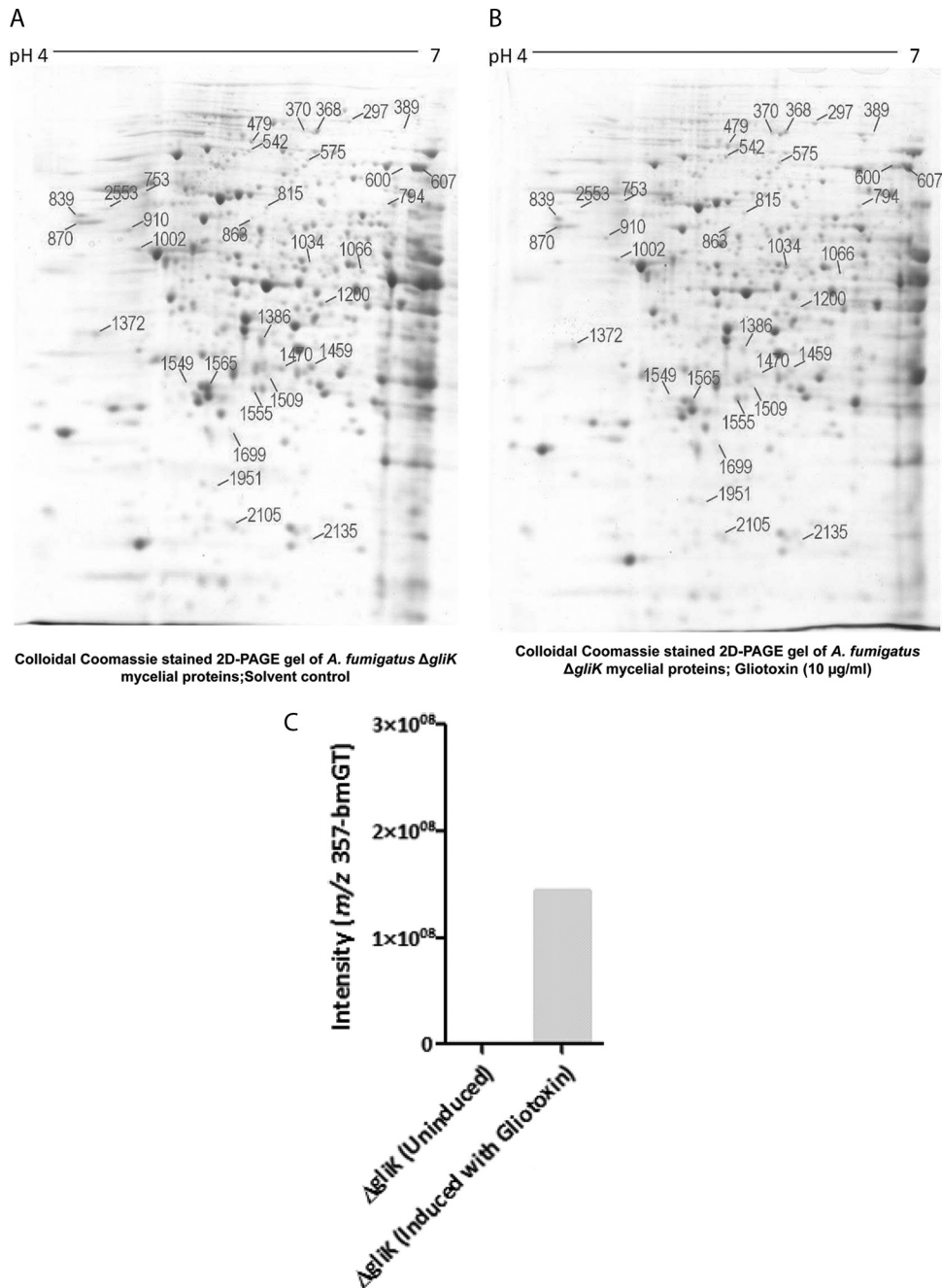


FIG 5 2D-PAGE analysis of the *A. fumigatus* Δ gliK strain. (A and B) Master 2D-PAGE of proteins with control treatment (A) or following exposure to gliotoxin (10 μ g/ml) for 4 h (B). Proteins were first separated on pH 4 to 7 strips, followed by SDS-PAGE. Proteins found to be significantly differentially expressed ($P < 0.05$) after analysis by using Progenesis SameSpot software are numbered. (C) *In vitro* GtmA activity, as determined by BmGT formation in the presence of SAM and GT-(SH)₂, is evident in mycelial lysates from *A. fumigatus* Δ gliK cells exposed to gliotoxin (5 μ g/ml for 3 h). Assay conditions were described previously (10). (D) Detection of a bis-glutathionylated gliotoxin biosynthetic intermediate (m/z 845.3) in mycelial lysates of the *A. fumigatus* Δ gliK strain.

teins with decreased abundance included ATP binding, nucleotide/nucleoside/nucleobase binding, and respiration. Data in [Table 4](#) confirm that GliT exhibits a highly significantly increased abundance (\log_2 fold change = 4.82; $P < 8.77 \times 10^{-5}$) in the *A. fumigatus* Δ gliG strain upon gliotoxin exposure. Interestingly, 10 additional proteins appear to be uniquely expressed in the *A. fumigatus* Δ gliG strain upon gliotoxin exposure, including a putative methyltransferase (AFUA_3G13140). Moreover, 8 proteins

exhibit significantly increased abundances, including GliN, a catalase-peroxidase (AFUA_8G1670), and an oxidoreductase (AFUA_1G01000). Although not statistically significant, the abundance of GtmA was also increased by \sim 5-fold upon gliotoxin exposure (data not shown). Exposure of the *A. fumigatus* Δ gliG strain to gliotoxin abolished the expression of 27 proteins, including 2 proteins (AFUA_8G00390 and AFUA_8G00440) encoded by the supercluster on chromosome 8 (40,

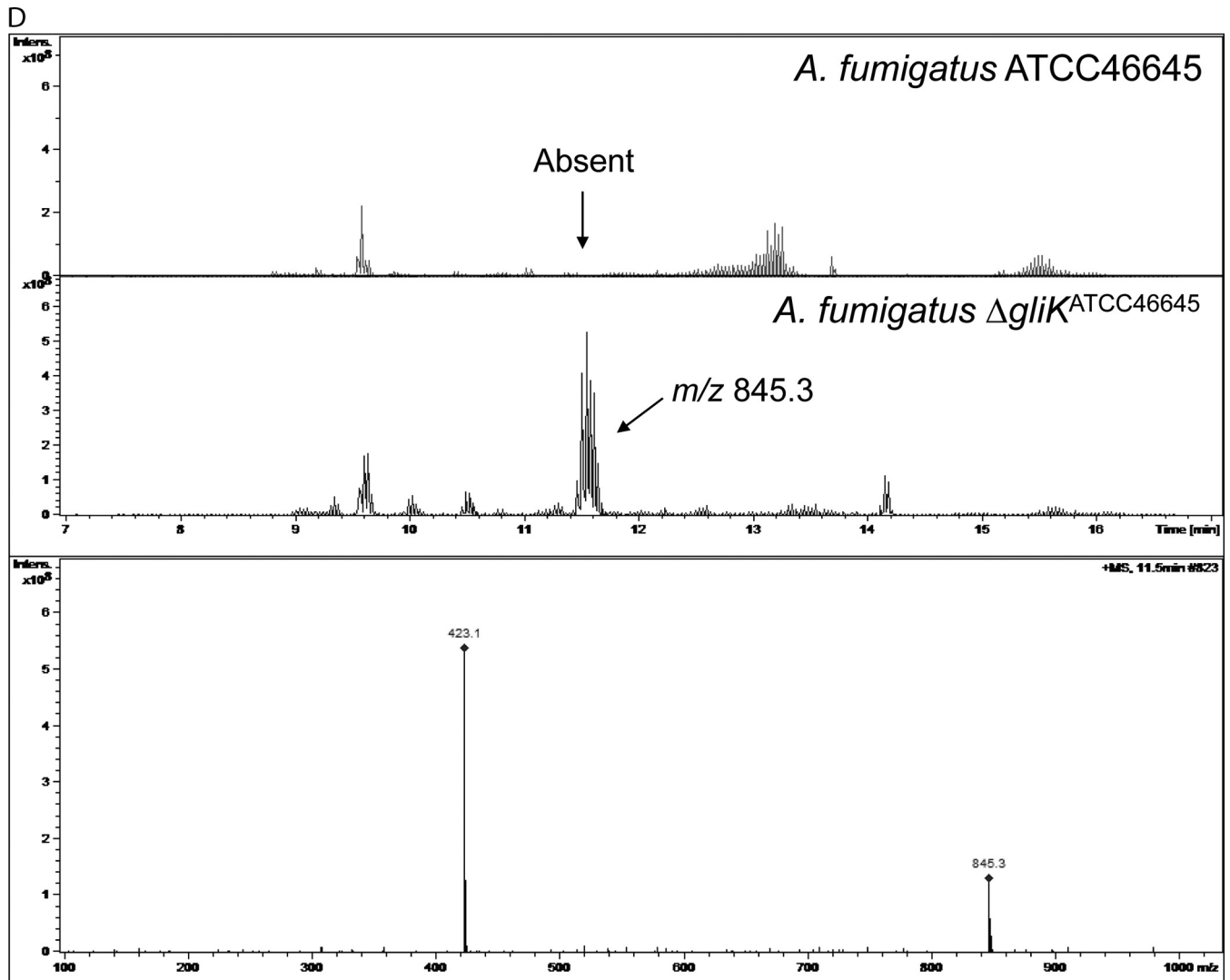


FIG 5 continued

41), and resulted in decreased abundances of 5 additional proteins (Table 5).

DISCUSSION

Here we reveal that deletion of *A. fumigatus gliA* completely disrupts the secretion of endogenous and exogenous gliotoxin, which results in the acquisition of a mild gliotoxin-sensitive phenotype but does not adversely affect BmGT formation or secretion. Moreover, it is revealed that elevated levels of endogenous gliotoxin induce transcriptome and proteomic changes in the *A. fumigatus* Δ *gliA* strain, including the induction of *gtmA* expression/GtmA abundance. We furthermore report that the *A. fumigatus* Δ *gliZ::* Δ *gliT* strain exhibits significantly greater resistance to gliotoxin than does the Δ *gliT* strain. This observation strongly suggests that an intact *de novo* gliotoxin biosynthesis pathway is necessary to effect maximum gliotoxin sensitivity, which engenders a highly deleterious situation in *A. fumigatus*. SAM depletion and SAH overproduction are most significant in the *A. fumigatus* Δ *gliT* strain, which suggests that GliT plays a critical role in preventing unrestricted GtmA-mediated GT-(SH)₂ bis-thiomethylation, which would

otherwise lead to a critical attenuation of the intracellular methylation capacity. Extensive transcriptomic and proteomic observations support the hypothesis that genes and proteins involved in the methyl/methionine cycle are overexpressed or have a significantly increased abundance, respectively, under conditions where either GliT is absent or its presence is significantly attenuated, as in the *A. fumigatus* Δ *gliK* strain upon gliotoxin exposure. Gliotoxin sensitivity has also been observed for an *A. fumigatus* Δ *metR* strain, which secretes BmGT (10) but exhibits impaired *gliT* induction upon exposure to gliotoxin. Thus, we now propose that *in vivo*, gliotoxin biosynthesis, resistance, and primary metabolism require regulation, via GliT and GliA functionality, to control gliotoxin oxidation and efflux, respectively, which in turn prevent SAM depletion and the concomitant overproduction of potentially inhibitory levels of SAH (Fig. 4A to C). We also conclude that bis-thiomethylation insufficiency is not primarily responsible for the gliotoxin sensitivity phenotype and that BmGT secretion occurs via an unknown, but GliA-independent, mechanism.

Wang et al. (15) convincingly reported that *gliA* deletion from

TABLE 2 Proteins undergoing a significant change in abundance in the *A. fumigatus* Δ *gliK* strain following exposure to gliotoxin (10 μ g/ml) relative to the solvent control^a

Protein	Fold change	Sequence coverage (%)	tM _r (Da)	CADRE identification no.	Spot
Proteins with increased abundance following gliotoxin addition					
Translation elongation factor eEF-3	↑ 5.6	8	117,768.4	AFUA_7G05660	297
Alanyl-tRNA synthetase	↑ 3.0	4	113,714.5	AFUA_8G03880	368
Eukaryotic translation initiation factor 3 subunit EifCb	↑ 2.7	5	85,065.4	AFUA_1G02030	542
Translation elongation factor G1	↑ 2.5	19	87,877.7	AFUA_4G08110	575
Heat shock protein Hsp98/Hsp104/ClpA	↑ 2.2	13	111,096.9	AFUA_1G15270	370
Glycine dehydrogenase	↑ 2.2	18	115,203.5	AFUA_4G03760	389
Cobalamin-independent methionine synthase MetH/D	↑ 2.2	5	87,736.8	AFUA_4G07360	607
Vesicular fusion protein Sec17	↑ 2.0	31	32,840.9	AFUA_2G12870	1699
CTP synthase	↑ 2.0	27	64,869.3	AFUA_7G05210	794
Cobalamin-independent methionine synthase MetH/D	↑ 1.9	14	87,736.8	AFUA_4G07360	600
Aminopeptidase	↑ 1.9	35	106,227.3	AFUA_4G09030	479
Alanine aminotransferase	↑ 1.9	31	55,135.5	AFUA_6G07770	1034
MTHFR	↑ 1.8	39	69,278.9	AFUA_2G11300	815
Mitochondrial processing peptidase alpha subunit, putative	↑ 1.7	8	63,997	AFUA_1G11870	863
Xanthine-guanine phosphoribosyl transferase Xpt1, putative	↑ 1.7	29	19,505.5	AFUA_4G04550	2105
Isochorismatase family hydrolase	↑ 1.7	26	20,904.6	AFUA_6G12220	2135
Pyruvate dehydrogenase complex component Pdx1	↑ 1.5	27	35,523.1	AFUA_3G08270	1509
GNAT family acetyltransferase	↑ 1.5	39	29,061.1	AFUA_5G00720	1951
Proteins with decreased abundance following gliotoxin addition					
Pyruvate dehydrogenase E1 component alpha subunit, putative	↓ 2.8	47	41,709.5	AFUA_1G06960	1200
Ran GTPase-activating protein 1 (RNA1 protein)	↓ 2.4	8	46,228.2	AFUA_3G07680	1002
Protein phosphatase 2a 65-kDa regulatory subunit	↓ 2.3	7	69,220	AFUA_1G05610	753
Diphthine synthase	↓ 2.1	24	31,492.2	AFUA_1G14020	1549
Homogentisate 1,2-dioxygenase (HmgA)	↓ 2.1	26	50,255.6	AFUA_2G04220	1066
Aspartic endopeptidase Pep2	↓ 2.1	20	43,355.1	AFUA_3G11400	1372
Zinc finger protein ZPR1	↓ 2.1	23	53,620	AFUA_6G10470	2553
CRAL/TRIO domain protein	↓ 2.0	27	46,169.8	AFUA_5G03690	910
Translation elongation factor EF2 subunit	↓ 1.9	11	93,428.8	AFUA_2G13530	1459
Thiamine biosynthesis protein (Nmt1)	↓ 1.9	38	38,323	AFUA_5G02470	1470
Oxidoreductase, 2OG-Fe(II) oxygenase family	↓ 1.8	13	43,013.2	AFUA_1G01000	1386
Nucleosome assembly protein Nap1	↓ 1.8	28	48,336.4	AFUA_5G05540	839
Protein disulfide isomerase Pdi1	↓ 1.6	31	56,187.2	AFUA_2G06150	870

^a A change in abundance was considered significant at a *P* value of <0.05. Protein identification was achieved by 2D-PAGE and LC-MS/MS. Statistical analysis was performed by using Student's *t* test. ↑ and ↓ indicate fold increases and decreases, respectively, in protein abundance upon exposure to gliotoxin (10 μ g/ml) relative to the solvent control. The CADRE gene identification number indicates *A. fumigatus* gene annotation nomenclature according to references 36 and 54. Spot indicates the number assigned to the protein in Fig. 5. tM_r, theoretical molecular mass; 2OG, 2-oxoglutarate.

A. fumigatus Afs35 led to significantly reduced secretion of gliotoxin, the acquisition of a gliotoxin-sensitive phenotype, significantly increased *gliZ* expression levels, and a reduction in intracellular gliotoxin levels. Wang et al. also noted elevated *gliT* expression in the *A. fumigatus* Δ *gliA* strain and overall concluded that *gliA*- and *gliT*-mediated self-protection were distinct mechanisms. Our data in part agree with those reported by Wang et al.; however, our distinct findings regarding elevated intracellular BmGT levels, that BmGT secretion remains intact, along with significant upregulation of *gtmA* expression by elevated intracellular gliotoxin levels, in the *A. fumigatus* Δ *gliA* strain lead us to alternative conclusions. In our model, we propose that *gliA* deletion results in elevated intracellular gliotoxin levels, which in turn induce *gliT* (as also observed previously [15]) along with *gtmA*, thereby increasing the formation, intracellular accumulation, and secretion of BmGT. Our hypothesis is in complete accordance with both of our data sets; however, it is based on the conclusion that

GliT and *GliA* work in concert, as opposed to by distinct mechanisms, to effect gliotoxin resistance in *A. fumigatus*. A novel C₂H₂ transcription factor that also regulates *gliA* expression, with *gliZ*, has been identified (42), which may also function to protect *A. fumigatus* against exogenous gliotoxin.

The absence of both *gliZ* and *gliT* from *A. fumigatus* results in a codeficiency in gliotoxin biosynthesis (43) and self-protection (12, 13) and leads to significantly improved resistance to exogenous gliotoxin compared to that observed for the *A. fumigatus* Δ *gliT* strain. This apparently puzzling result means that the growth-inhibitory phenotype observed upon gliotoxin exposure requires both a functional biosynthetic system and an inactive resistance system. Otherwise, if *gliZ* expression is intact, exogenous gliotoxin induces *gli* cluster expression (13, 16, 17) and leads to the *de novo* production of GT-(SH)₂ and thus an exacerbation of the growth-inhibitory effect of exogenous gliotoxin. This observation also explains why the *A. fumigatus* Δ *gliT* strain grows

TABLE 3 LFQ proteomics analysis of proteins with increased abundance in, or that are or unique to, the *A. fumigatus* $\Delta gliK^{ATCC 26933}$ strain with gliotoxin compared to the $\Delta gliK^{ATCC 26933}$ strain with methanol^a

Protein description	Log ₂ -fold increase	P value	No. of peptides	Sequence coverage (%)	CADRE identification no.
Ortholog of <i>A. nidulans</i> FGSC A4 protein AN9303, <i>Aspergillus niger</i> CBS 513.88 protein An07g06460, <i>Aspergillus oryzae</i> RIB40 protein AO090023000147, and <i>Neosartorya fischeri</i> NRRL 181 protein NFIA_064190	Unique	NA	9	40.4	AFUA_3G13140
Protein with domain(s) with predicted catalytic activity, coenzyme binding, nucleotide binding activity, and role in cellular metabolic processes	Unique	NA	3	12.6	AFUA_4G02810
Putative aldehyde reductase with higher expression levels in biofilm grown for 48 h than in planktonic cells; repressed by gliotoxin exposure	Unique	NA	15	65	AFUA_5G02020
Putative <i>p</i> -nitroreductase family protein; protein induced by heat shock; Yap1-dependent induction in response to hydrogen peroxide; induced by gliotoxin exposure	Unique	NA	3	22.1	AFUA_5G09910
Protein with domain(s) with predicted hydrolase activity	Unique	NA	5	28	AFUA_5G12770
Ortholog of <i>A. nidulans</i> FGSC A4 protein AN1460, <i>A. niger</i> CBS 513.88 protein An16g08480, and <i>A. oryzae</i> RIB40 protein AO090023000335	Unique	NA	7	45.4	AFUA_8G04510
Gliotoxin bis-thiomethyltransferase GtmA ^b	Unique	NA	4	25.2	AFUA_2G11120
Protein with ortholog(s) that has homoserine <i>O</i> -acetyltransferase activity and role in cysteine metabolic processes	Unique	NA	2	6.6	AFUA_5G08600
Protein with domain(s) with predicted nucleotide binding and oxidoreductase activities and role in metabolic processes	Unique	NA	7	61.3	AFUA_5G14000
Protein with domain(s) with predicted hydrolase activity, acting on activity of ester bonds	Unique	NA	5	20.7	AFUA_7G04910
Protein with domain(s) with predicted carbonate dehydratase activity, zinc ion binding activity, and role in carbon utilization	Unique	NA	4	40.9	AFUA_8G06554
Gliotoxin oxidoreductase required for gliotoxin biosynthesis; encoded by the gliotoxin biosynthetic gene cluster; involved in self-protection against exogenous gliotoxin; induced in biofilm; immunoreactive (GliT)	3.837	3.39E-02	13	71.3	AFUA_6G09740
Protein with domain(s) with predicted kynureninase activity, pyridoxal phosphate binding activity; role in NAD biosynthetic processes and tryptophan catabolic processes; cytoplasm localization	2.221	1.43E-03	16	55.6	AFUA_4G09840
Glyceraldehyde-3-phosphate dehydrogenase, putative	1.956	1.10E-02	24	74.5	AFUB_049500
Putative bifunctional catalase-peroxidase	1.945	1.00E-04	26	54.4	AFUA_8G01670
Putative integral plasma membrane heat shock protein	1.900	1.24E-02	6	58.5	AFUA_6G06470
Protein with domain(s) with predicted acid amino acid ligase activity and role in posttranslational protein modification	1.391	2.93E-03	2	20.7	AFUA_3G14430
Protein with domain(s) with predicted catalytic activity and role in metabolic processes	1.338	4.53E-02	7	21.9	AFUA_3G09240
Glyoxylase family protein, putative	1.335	1.89E-02	3	16.9	AFUB_090580
Protein with ortholog(s) that has protein binding and bridging activity and roles in actin cortical patch assembly, axial cellular bud site selection, bipolar cellular bud site selection, and endocytosis	1.286	1.37E-03	4	4.7	AFUA_7G03870
Putative 30-kDa heat shock protein; conidium-enriched protein	1.278	1.23E-02	6	38.3	AFUA_3G14540
Protein with ortholog(s) that has cytoplasmic stress granule localization	1.274	2.98E-03	2	17.7	AFUA_6G02450
Protein of unknown function; transcript upregulated in conidia exposed to neutrophils	1.247	3.99E-02	2	9.1	AFUA_1G11480
Putative myoinositol-phosphate synthase; transcript upregulated in conidia exposed to neutrophils	1.053	2.33E-04	21	60.3	AFUA_2G01010
Putative tripeptidyl-peptidase of the sedolisin family; predicted signal sequence for secretion	1.051	9.37E-03	11	27.6	AFUA_4G14000

^a Data are sorted by fold change, in descending order. Statistical analysis was performed by using Student's *t* test.

^b See reference 10.

normally in the absence of exogenous gliotoxin (12, 13). Thus, growth of the *A. fumigatus* $\Delta gliT$ strain is inhibited only by exogenous gliotoxin, which induces *gli* cluster activity (13, 17), because in the absence of GliT-mediated oxidation, gliotoxin cannot be secreted via GliA and so persists in the cell. We propose that the

additional presence of endogenous GT-(SH)₂, combined with that formed intracellularly upon the reduction of exogenous gliotoxin, results in SAM depletion and SAH overproduction as a consequence of GtmA activity, which in turn contributes to growth inhibition of the *A. fumigatus* $\Delta gliT$ strain. This further

TABLE 4 LFQ proteomics analysis of proteins with increased abundance in, or that are unique to, the *A. fumigatus* Δ gliG^{Af293} strain with gliotoxin compared to methanol-only exposure^a

Protein description	Log ₂ -fold increase	P value	No. of peptides	Sequence coverage (%)	CADRE identification no.
GNAT family N-acetyltransferase, putative	Unique		5	38.9	AFUA_3G00870
Putative uncharacterized protein	Unique		5	23.7	AFUA_6G12780
Methyltransferase, putative	Unique		10	42.4	AFUA_3G13140
Putative uncharacterized protein	Unique		2	10.7	AFUA_6G02010
Guanyl-nucleotide exchange factor (Sec7)	Unique		5	3	AFUA_7G05700
NADH-dependent flavin oxidoreductase	Unique		3	14.5	AFUA_7G06420
Aspartyl-tRNA synthetase, cytoplasmic	Unique		2	2.7	AFUA_1G02570
Putative uncharacterized protein	Unique		2	11.4	AFUA_4G07680
Nucleoporin SONB, putative	Unique		3	1.9	AFUA_4G11070
Nuclear and cytoplasmic polyadenylated RNA binding protein Pub1	Unique		4	7.8	AFUA_1G12000
Gliotoxin oxidoreductase (GliT)	4.825	8.77E-05	19	66.5	AFUA_6G09740
Catalase-peroxidase	3.725	0.000676	42	75.2	AFUA_8G01670
Oxidoreductase, 2OG-Fe(II) oxygenase family	3.507	0.020389	9	34	AFUA_1G01000
N-Methyltransferase (GliN)	2.561	0.00636	6	28.4	AFUA_6G09720
Short-chain dehydrogenase, putative	1.781	0.014034	13	68.3	AFUA_4G08710
Heat shock protein Hsp30-like, putative	1.558	0.026821	5	43	AFUA_6G06470
Putative uncharacterized protein	1.549	0.008346	10	68.2	AFUA_3G00960
Lipase/esterase, putative	1.549	0.00262	7	32.7	AFUA_1G15430
Class V chitinase, putative	1.287	0.002555	7	27.8	AFUA_3G11280

^a Data are sorted by fold change, in descending order. Statistical analysis was performed by using Student's *t* test.

underpins our hypothesis that *bis*-thiomethylation of gliotoxin is not a backup strategy mediated by GliM or GliN, as has been proposed for *A. fumigatus* (14), but serves to negatively regulate gliotoxin biosynthesis via the non-*gli* cluster gene *gtmA* (10). In the absence of *gliT* and in the presence of exogenous gliotoxin, this negative regulatory system causes a dysregulation of SAM:SAH homeostasis (Fig. 6).

Cellular SAM and SAH levels were also significantly decreased and increased, respectively ($P = 0.0106$ and $P = 0.0390$, respectively) in the *A. fumigatus* Δ gliG strain (Fig. 4C), which was previously shown to be resistant to the growth-inhibitory effects of exogenous gliotoxin (4); however, cellular SAM levels were comparable to those in Af293 exposed to exogenous gliotoxin. This finding suggests that the Δ gliG strain retains the ability to maintain cellular SAM levels consistent with those in the wild type upon exogenous gliotoxin exposure, unlike other *gli* mutants, and consequently is resistant to the growth-inhibitory effects. GliG mediates the conjugation of glutathione (GSH) to a gliotoxin biosynthetic intermediate during synthesis (4, 18, 44, 45). This reaction is effectively inhibited in the Δ gliG strain; thus, it is possible that in the Δ gliG strain, surplus GSH can be converted to Hcy and, consequently, SAM through the transsulfuration process, accounting for the maintenance of cellular SAM levels upon the addition of exogenous gliotoxin. It has been shown that a number of methylated gliotoxin-related intermediates/shunt metabolites are present in *A. fumigatus*, which are absent in the *A. fumigatus* Δ gliZ strain (9). We hypothesized that if gliotoxin could induce *gli* cluster expression in the *A. fumigatus* Δ gliZ strain (i.e., independently of *gliZ*), the production of these intermediates could lead to SAM depletion and SAH production. However, the addition of gliotoxin to the *A. fumigatus* Δ gliZ strain did not induce gliotoxin biosynthesis and secretion, as ¹³C-labeled gliotoxin was undetectable in *A. fumigatus* Δ gliZ culture supernatants following feeding experiments with [¹³C]phenylalanine (data not shown). However, SAM depletion and SAH production were evident in the *A.*

fumigatus Δ gliZ strain upon exposure to exogenous gliotoxin (Fig. 4C).

The addition of gliotoxin significantly upregulates the expression of genes involved in the methyl/methionine cycle in the *A. fumigatus* Δ gliT strain (17) (see Table S3 in the supplemental material). As shown here, significantly elevated SAH levels are also uniquely observed in this strain in response to gliotoxin exposure. Methionine produced from Hcy can either be used in protein synthesis or, alternatively, enter the methionine cycle, whereby it is S-adenylated to form SAM (37). SAM is a ubiquitous cellular methyl donor and is utilized by methyltransferases for DNA, protein, and metabolite methylation reactions (46). Elevated SAH levels prevent the production of toxic Hcy (26) and may lead to the inhibition of cellular methyltransferases via competitive inhibition of SAM binding. Our data are consistent with a scenario whereby exogenous and *de novo*-produced gliotoxin undergoes *bis*-thiomethylation in an unregulated manner in the absence of GliT, leading to elevated SAH and attenuated SAM levels, respectively, which activate the methyl/methionine cycle to increase the SAM supply (Fig. 6). Interestingly, in the *A. fumigatus* Δ metR strain, the addition of cystathionine potentiates gliotoxin sensitivity, even though the mutant is not significantly sensitive to the addition of cystathionine alone, compared to ATCC 46645. Cystathionine feeds into the methyl/methionine cycle, which suggests that increased levels of cycle components, in conjunction with upregulated methyl/methionine cycle genes due to the addition of gliotoxin, exacerbate gliotoxin sensitivity. Indeed, it was reported recently that SAM depletion in mammalian cells can induce cell cycle arrest in the G₁ phase (47).

Comparative 2D-PAGE-LC-MS/MS analysis of mycelial protein extracts of the *A. fumigatus* Δ gliK strain, which is partially sensitive to exogenous gliotoxin (7), revealed a significantly increased abundance of cobalamin-independent methionine synthase (MetH) (present in two protein spots, with 1.9- and 2.2-fold-increased abundances, respectively). MetH couples

TABLE 5 LFQ proteomics analysis of proteins with decreased abundance in, or that are absent from, the *A. fumigatus* $\Delta gliG^{AF293}$ strain with gliotoxin compared to methanol-only exposure^a

Protein description	Log ₂ -fold decrease	P value	No. of peptides	Sequence coverage (%)	CADRE identification no.
Putative uncharacterized protein	Absent		7	8.4	AFUA_2G05520
Alternative oxidase	Absent		4	12.5	AFUA_2G05060
Putative uncharacterized protein	Absent		3	11.9	AFUA_6G13500
ATP-dependent RNA helicase Mss116, mitochondrial	Absent		3	6.6	AFUA_1G15620
Ferrochelatase	Absent		3	8.9	AFUA_5G07750
tRNA [adenine(58)-N(1)]-methyltransferase catalytic subunit Trm61	Absent		2	5.8	AFUA_5G09620
Mitochondrial phosphate carrier protein, putative	Absent		4	9.2	AFUA_3G08430
Catalase	Absent		4	12.5	AFUA_2G18030
U6 snRNA-associated Sm-like protein LSM4, putative	Absent		3	31.1	AFUA_2G12020
Regulator of nonsense transcripts, putative	Absent		3	4	AFUA_1G13060
Mitochondrial molecular chaperone (Atp12), putative	Absent		5	16	AFUA_7G02490
O-Methyltransferase, putative	Absent		3	27	AFUA_8G00390
Steroid monooxygenase, putative	Absent		3	6.3	AFUA_8G00440
tRNA-guanine transglycosylase family protein	Absent		3	8.5	AFUA_5G03470
Ubiquitin-conjugating enzyme (UbcH), putative	Absent		3	42.8	AFUA_5G04060
snRNP and snoRNP protein (Snu13), putative	Absent		2	28.6	AFUA_2G05950
Cellular morphogenesis regulator DopA	Absent		3	1.4	AFUA_2G05020
GTP binding protein, putative	Absent		7	24.7	AFUA_1G05560
Putative uncharacterized protein	Absent		3	17.8	AFUA_6G09950
mRNA splicing factor (Prp17), putative	Absent		3	9.5	AFUA_6G07300
Alpha,alpha-trehalase TreB/Nth1	Absent		4	5.9	AFUA_4G13530
Hsp70 family protein	Absent		2	3.3	AFUA_1G15200
RNase III domain protein	Absent		2	6.2	AFUA_5G09670
Putative uncharacterized protein	Absent		3	10.9	AFUA_3G10710
DNA replication licensing factor Mcm2, putative	Absent		4	5.8	AFUA_3G14010
Nuclear cohesin complex subunit (Psc3), putative	Absent		4	4	AFUA_2G16080
Cyclic AMP-dependent protein kinase catalytic subunit PkaC1	Absent		3	10.6	AFUA_2G12200
L-Amino acid oxidase LaoA	-1.198	0.026668	14	28	AFUA_7G06810
40S ribosomal protein S25, putative	-1.300	0.048129	9	51.6	AFUA_1G16523
DUF636 domain protein	-1.348	0.049468	6	81.6	AFUA_2G15290
Hydrophobin RodA	-3.345	0.013418	3	31.4	AFUA_5G09580
Aldehyde dehydrogenase, putative	-3.410	0.04575	15	51.3	AFUA_7G01000

^a Data are sorted by fold change, in descending order. Statistical analysis was performed by using Student's *t* test.

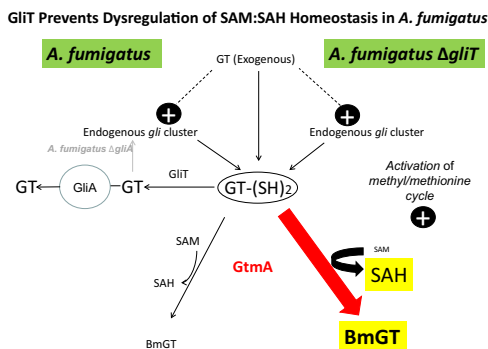


FIG 6 GliT prevents dysregulation of SAM:SAH homeostasis in *A. fumigatus*. This model is in accordance with all experimental observations whereby exogenous and/or endogenous gliotoxin results in GT-(SH)₂ formation followed by conversion to gliotoxin and secretion via GliA. Alternatively, GT-(SH)₂ can be converted to BmGT via GtmA under controlled conditions (10, 20, 53). In the absence of GliT ($\Delta gliT$), GtmA-mediated BmGT formation at nonphysiological levels of occurs, leading to SAM depletion and SAH overproduction. In the *A. fumigatus* $\Delta gliA$ strain, increases in gli cluster activity and GtmA abundance also occur, leading to elevated intra- and extracellular BmGT levels. Note that because the absence of GliT is so deleterious (53), the attenuated levels of GliT present in the *A. fumigatus* $\Delta gliK$ strain provided an alternative experimental system to reveal the link to the methyl/methionine cycle (Tables 2 and 3; see also Fig. S3 in the supplemental material).

the methyl cycle and the methionine cycle through the methylation of Hcy and the subsequent regeneration of tetrahydrofolate (THF) (see Fig. S3 in the supplemental material). An additional step in the methyl cycle, involving the conversion of THF to 5,10-methylene-THF, is usually catalyzed by SHMT, with the simultaneous metabolism of serine and formation of glycine (48). However, in the presence of excess glycine or a limited pool of 5,10-methylene-THF, this step can be catalyzed by the mitochondrial glycine decarboxylase complex (GDC) (49). The abundance of a subunit of this complex, glycine dehydrogenase (see Fig. S3 in the supplemental material), was also increased in the *A. fumigatus* $\Delta gliK$ strain following incubation with gliotoxin (2.2-fold; $P = 0.025$), suggesting an overall upregulation of the methyl cycle in the *A. fumigatus* $\Delta gliK$ strain upon gliotoxin exposure. MetH has also been shown to be a target of the transcriptional activator *yap1* in *A. fumigatus*, and expression of this protein is induced in the presence of oxidative stress (50). In fungi, the production of methionine from Hcy is catalyzed by MetH/D, and in *Candida albicans*, this enzyme has been shown to be essential for cell viability (37). Indeed, Hcy induces the upregulation of *A. nidulans* methionine synthase (51), in addition to the positive regulation of MTHFR/MtrA expression (38). Interestingly, a significantly increased abundance of MTHFR/MtrA

was observed in gliotoxin-exposed $\Delta gliK$ cells (1.8-fold; $P < 0.05$). This scenario is in contrast to that observed for wild-type *A. fumigatus*, whereby downregulation of MTHFR/MtrA was noted in response to gliotoxin and H_2O_2 combined, relative to the solvent control (11). Although an altered GliT abundance was not detectable in the *A. fumigatus* $\Delta gliK$ strain during the above-mentioned 2-DE-LC-MS/MS analysis, it has been reported that elevated *gliT* expression occurs in response to gliotoxin exposure in this mutant (7). Here, parallel LFQ proteomic investigations of the *A. fumigatus* $\Delta gliK$ strain, in the presence and absence of gliotoxin, revealed a 14- to 15-fold (\log_2 -fold change = 3.837)-increased abundance of GliT, compared to the 250-fold increase in wild-type *A. fumigatus* following gliotoxin exposure. Thus, we hypothesize that the apparent gliotoxin sensitivity of the *A. fumigatus* $\Delta gliK$ strain (7) can in part be explained by the attenuated expression of GliT, compared to that of the wild type, and a consequent deficit in gliotoxin secretion, as noted by the authors of that study.

Figure 6 presents a model for how GliT prevents dysregulation of SAM:SAH homeostasis in *A. fumigatus*. GT-(SH)₂ formation (10) is mediated by *gli* cluster activity, which in turn is induced by gliotoxin. GT-(SH)₂ is either oxidized to gliotoxin by GliT, followed by GliA-mediated secretion, or converted to BmGT by the SAM-dependent activity of GtmA. Notably, GT-(SH)₂ dismutation to BmGT consumes 2 SAM molecules. BmGT is secreted from *A. fumigatus*; concomitantly, its biosynthesis results in SAM depletion and SAH formation. Under normal circumstances, SAH is reconverted to SAM via the methionine cycle, which in turn necessitates the activity of the methyl cycle (Fig. 6; see also Fig. S3 in the supplemental material). Thus, GtmA appears to link the regulation of gliotoxin biosynthesis to what are conventionally considered to be primary metabolic processes. In doing so, a highly precarious situation materializes in *A. fumigatus*, whereby any scenario which increases GT-(SH)₂ levels (e.g., *gliT* deletion) could potentially lead to SAM depletion and SAH overproduction and the subsequent occurrence of unwanted downstream consequences. Regulation of gliotoxin biosynthesis is indeed a high-risk strategy for *A. fumigatus* and has necessitated the evolution, and integration, of multiple facilitatory mechanisms to prevent deleterious eventualities.

Finally, it has been proposed that epigenetic modifications, including methylation, may affect cellular metabolism by limiting SAM availability for essential reactions (52). Conversely, it has not escaped our attention that SAM limitation as a consequence of excessive BmGT formation could impact the epigenetic regulation of chromatin structure and secondary metabolite formation, especially since altered fumagillin, pseurotin A, and brevianamide F levels have been observed in the *A. fumigatus* $\Delta gliT$ strain (17).

ACKNOWLEDGMENTS

This work was funded by a Science Foundation Ireland Principal Investigator award to S.D. (PI/11/1188). R.A.O. was funded by a 3U Partnership award (DCU/NUIM/RCSI). S.H. and S.K.D. are recipients of Irish Research Council Embark Ph.D. fellowships. LC-MS facilities were funded by competitive awards from Science Foundation Ireland (12/RI/2346 [3]) and the Irish Higher Education Authority. qRT-PCR instrumentation was funded by Science Foundation Ireland (SFI/07/RFP/GEN/F571/ECO7).

The image station for the visualization of Southern blots was funded by Science Foundation Ireland career development award 13/CDA/2142 to Ozgur Bayram.

REFERENCES

- Gerken T, Walsh CT. 2013. Cloning and sequencing of the chaetocin biosynthetic gene cluster. *Chembiochem* 14:2256–2258. <http://dx.doi.org/10.1002/cbic.201300513>.
- Chang S-L, Chiang Y-M, Yeh H-H, Wu T-K, Wang CCC. 2013. Reconstitution of the early steps of gliotoxin biosynthesis in *Aspergillus nidulans* reveals the role of the monooxygenase GliC. *Bioorg Med Chem Lett* 23:2155–2157. <http://dx.doi.org/10.1016/j.bmcl.2013.01.099>.
- Guo CJ, Yeh HH, Chiang YM, Sanchez JF, Chang SL, Bruno KS, Wang CC. 2013. Biosynthetic pathway for the epipolythiodioxopiperazine acetylaranotin in *Aspergillus terreus* revealed by genome-based deletion analysis. *J Am Chem Soc* 135:7205–7213. <http://dx.doi.org/10.1021/ja3123653>.
- Davis C, Carberry S, Schrettl M, Singh I, Stephens JC, Barry SM, Kavanagh K, Challis GL, Brougham D, Doyle S. 2011. The role of glutathione S-transferase GliG in gliotoxin biosynthesis in *Aspergillus fumigatus*. *Chem Biol* 18:542–552. <http://dx.doi.org/10.1016/j.chembiol.2010.12.022>.
- Scharf DH, Chankhamjon P, Scherlach K, Heinekamp T, Willing K, Brakhage AA, Hertweck C. 2013. Epidithiodiketopiperazine biosynthesis: a four-enzyme cascade converts glutathione conjugates into transannular disulfide bridges. *Angew Chem Int Ed Engl* 52:11092–11095. <http://dx.doi.org/10.1002/anie.201305059>.
- Choi HS, Shim JS, Kim J-A, Kang SW, Kwon HJ. 2007. Discovery of gliotoxin as a new small molecule targeting thioredoxin redox system. *Biochem Biophys Res Commun* 359:523–528. <http://dx.doi.org/10.1016/j.bbrc.2007.05.139>.
- Gallagher L, Owens RA, O’Keeffe G, Dolan SK, Schrettl M, Kavanagh K, Jones G, Doyle S. 2012. The *Aspergillus fumigatus* protein GliK protects against oxidative stress and is essential for gliotoxin biosynthesis. *Eukaryot Cell* 11:1226–1238. <http://dx.doi.org/10.1128/EC.00113-12>.
- Domingo MP, Colmenarejo C, Martínez-Lostao L, Müllbacher A, Jarne C, Revillo MJ, Delgado P, Roc L, Meis JF, Rezusta A, Pardo J, Gálvez EM. 2012. Bis(methyl)gliotoxin proves to be a more stable and reliable marker for invasive aspergillosis than gliotoxin and suitable for use in diagnosis. *Diagn Microbiol Infect Dis* 73:57–64. <http://dx.doi.org/10.1016/j.diagmicrobio.2012.01.012>.
- Forseth RR, Fox EM, Chung D, Howlett BJ, Keller NP, Schroeder FC. 2011. Identification of cryptic products of the gliotoxin gene cluster using NMR-based comparative metabolomics and a model for gliotoxin biosynthesis. *J Am Chem Soc* 133:9678–9681. <http://dx.doi.org/10.1021/ja2029987>.
- Dolan SK, Owens RA, O’Keeffe G, Hammel S, Fitzpatrick DA, Jones GW, Doyle S. 2014. Regulation of non-ribosomal peptide synthesis: bis-thiomethylation attenuates gliotoxin biosynthesis in *Aspergillus fumigatus*. *Chem Biol* 21:999–1012. <http://dx.doi.org/10.1016/j.chembiol.2014.07.006>.
- Owens RA, Hammel S, Sheridan KJ, Jones GW, Doyle SA. 2014. Proteomic approach to investigating gene cluster expression and secondary metabolite functionality in *Aspergillus fumigatus*. *PLoS One* 9:e106942. <http://dx.doi.org/10.1371/journal.pone.0106942>.
- Scharf DH, Remme N, Heinekamp T, Hortschansky P, Brakhage AA, Hertweck C. 2010. Transannular disulfide formation in gliotoxin biosynthesis and its role in self-resistance of the human pathogen *Aspergillus fumigatus*. *J Am Chem Soc* 132:10136–10141. <http://dx.doi.org/10.1021/ja103262m>.
- Schrettl M, Carberry S, Kavanagh K, Haas H, Jones GW, O’Brien J, Nolan A, Stephens J, Fenelon O, Doyle S. 2010. Self-protection against gliotoxin—a component of the gliotoxin biosynthetic cluster, GliT, completely protects *Aspergillus fumigatus* against exogenous gliotoxin. *PLoS Pathog* 6:e1000952. <http://dx.doi.org/10.1371/journal.ppat.1000952>.
- Li B, Forseth RR, Bowers AA, Schroeder FC, Walsh CT. 2012. A backup plan for self-protection: S-methylation of holomycin biosynthetic intermediates in *Streptomyces clavuligerus*. *Chembiochem* 13:2521–2526. <http://dx.doi.org/10.1002/cbic.201200536>.
- Wang D, Toyotome T, Muraosa Y, Watanabe A, Wuren T, Bunsupa S, Aoyagi K, Yamazaki M, Takino M, Kamei K. 2014. GliA in *Aspergillus fumigatus* is required for its tolerance to gliotoxin and affects the amount

- of extracellular and intracellular gliotoxin. *Med Mycol* 52:506–518. <http://dx.doi.org/10.1093/mmy/myu007>.
16. Cramer RA, Gamcsik MP, Brooking RM, Najvar LK, Kirkpatrick WR, Patterson TF, Balibar CJ, Graybill JR, Perfect JR, Abraham SN, Steinbach WJ. 2006. Disruption of a nonribosomal peptide synthetase in *Aspergillus fumigatus* eliminates gliotoxin production. *Eukaryot Cell* 5:972–980. <http://dx.doi.org/10.1128/EC.00049-06>.
 17. O’Keeffe G, Hammel S, Owens RA, Keane TM, Fitzpatrick DA, Jones GW, Doyle S. 2014. RNA-seq reveals the pan-transcriptomic impact of attenuating the gliotoxin self-protection mechanism in *Aspergillus fumigatus*. *BMC Genomics* 15:894. <http://dx.doi.org/10.1186/1471-2164-15-894>.
 18. Scharf DH, Remme N, Habel A, Chankhamjon P, Scherlach K, Heinekamp T, Hortschansky P, Brakhage AA, Hertweck C. 2011. A dedicated glutathione S-transferase mediates carbon-sulfur bond formation in gliotoxin biosynthesis. *J Am Chem Soc* 133:12322–12325. <http://dx.doi.org/10.1021/ja201311d>.
 19. Scharf DH, Chankhamjon P, Scherlach K, Heinekamp T, Roth M, Brakhage AA, Hertweck C. 2012. Epidithiol formation by an unprecedented twin carbon-sulfur lyase in the gliotoxin pathway. *Angew Chemie Int Ed Engl* 51:10064–10068. <http://dx.doi.org/10.1002/anie.201205041>.
 20. Scharf DH, Habel A, Heinekamp T, Brakhage AA, Hertweck C. 2014. Opposed effects of enzymatic gliotoxin N- and S-methylations. *J Am Chem Soc* 136:11674–11679. <http://dx.doi.org/10.1021/ja5033106>.
 21. Owens RA, O’Keeffe G, O’Hanlon KA, Gallagher L, Doyle S. 2014. Virulence characteristics of *Aspergillus fumigatus*, p 163–194. In Sullivan DJ, Moran GP (ed), *Human pathogenic fungi: molecular biology and pathogenic mechanisms*. Caister Academic Press, Norfolk, United Kingdom.
 22. Amich J, Schafferer L, Haas H, Krappmann S. 2013. Regulation of sulphur assimilation is essential for virulence and affects iron homeostasis of the human-pathogenic mould *Aspergillus fumigatus*. *PLoS Pathog* 9:e1003573. <http://dx.doi.org/10.1371/journal.ppat.1003573>.
 23. Brzywczy J, Kacprzak MM, Paszewski A. 2011. Novel mutations reveal two important regions in *Aspergillus nidulans* transcriptional activator MetR. *Fungal Genet Biol* 48:104–112. <http://dx.doi.org/10.1016/j.fgb.2010.10.002>.
 24. Sauter M, Moffatt B, Saechao MC, Hell R, Wirtz M. 2013. Methionine salvage and S-adenosylmethionine: essential links between sulfur, ethylene and polyamine biosynthesis. *Biochem J* 451:145–154. <http://dx.doi.org/10.1042/BJ20121744>.
 25. Dorgan KM, Wooderchak WL, Wynn DP, Karschner EL, Alfaro JF, Cui Y, Zhou ZS, Hevel JM. 2006. An enzyme-coupled continuous spectrophotometric assay for S-adenosylmethionine-dependent methyltransferases. *Anal Biochem* 350:249–255. <http://dx.doi.org/10.1016/j.ab.2006.01.004>.
 26. Sienko M, Natorff R, Owczarek S, Olewiecki I, Paszewski A. 2009. *Aspergillus nidulans* genes encoding reverse transsulfuration enzymes belong to homocysteine regulon. *Curr Genet* 55:561–570. <http://dx.doi.org/10.1007/s00294-009-0269-3>.
 27. Nielsen ML, Albertsen L, Lettier G, Nielsen JB, Mortensen UH. 2006. Efficient PCR-based gene targeting with a recyclable marker for *Aspergillus nidulans*. *Fungal Genet Biol* 43:54–64. <http://dx.doi.org/10.1016/j.fgb.2005.09.005>.
 28. Kubodera T, Yamashita N, Nishimura A. 2000. Pyriithiamine resistance gene (*ptrA*) of *Aspergillus oryzae*: cloning, characterization and application as a dominant selectable marker for transformation. *Biosci Biotechnol Biochem* 64:1416. <http://dx.doi.org/10.1271/bbb.64.1416>.
 29. O’Keeffe G, Jöchl C, Kavanagh K, Doyle S. 2013. Extensive proteomic remodeling is induced by eukaryotic translation elongation factor 1B γ deletion in *Aspergillus fumigatus*. *Protein Sci* 22:1612–1622. <http://dx.doi.org/10.1002/pro.2367>.
 30. O’Hanlon KA, Cairns T, Stack D, Schrettl M, Bignell EM, Kavanagh K, Miggins SM, O’Keeffe G, Larsen TO, Doyle S. 2011. Targeted disruption of nonribosomal peptide synthetase *pes3* augments the virulence of *Aspergillus fumigatus*. *Infect Immun* 79:3978–3992. <http://dx.doi.org/10.1128/IAI.00192-11>.
 31. Roeder S, Dreschler K, Wirtz M, Cristescu SM, van Harren FJM, Hell R, Piechulla B. 2009. SAM levels, gene expression of SAM synthetase, methionine synthase and ACC oxidase, and ethylene emission from *N. suaveolens* flowers. *Plant Mol Biol* 70:535–546. <http://dx.doi.org/10.1007/s11103-009-9490-1>.
 32. Zhou J, Waszkuc T, Garbis S, Mohammed F. 2002. Liquid chromatographic determination of S-adenosyl-L-methionine in dietary supplement tablets. *J AOAC Int* 85:901–905.
 33. Collins C, Keane TM, Turner DJ, O’Keeffe G, Fitzpatrick DA, Doyle S. 2013. Genomic and proteomic dissection of the ubiquitous plant pathogen, *Armillaria mellea*: toward a new infection model system. *J Proteome Res* 12:2552–2570. <http://dx.doi.org/10.1021/pr301131t>.
 34. Cox J, Mann M. 2008. MaxQuant enables high peptide identification rates, individualized p.p.b.-range mass accuracies and proteome-wide protein quantification. *Nat Biotechnol* 26:1367–1372. <http://dx.doi.org/10.1038/nbt.1511>.
 35. Priebe S, Linde J, Albrecht D, Guthke R, Brakhage AA. 2011. FungiFun: a Web-based application for functional categorization of fungal genes and proteins. *Fungal Genet Biol* 48:353–358. <http://dx.doi.org/10.1016/j.fgb.2010.11.001>.
 36. Nierman WC, Pain A, Anderson MJ, Wortman JR, Kim HS, Arroyo J, Berriman M, Abe K, Archer DB, Bermejo C, Bennett J, Bowyer P, Chen D, Collins M, Coulson R, Davies R, Dyer PS, Farman M, Fedorova N, Fedorova N, Feldblyum TV, Fischer R, Fosker N, Fraser A, García JL, García MJ, Goble A, Goldman GH, Gomi K, Griffith-Jones S, Gwilliam R, Haas B, Haas H, Harris D, Horiuchi H, Huang J, Humphray S, Jiménez J, Keller N, Khouri H, Kitamoto K, Kobayashi T, Konzack S, Kulkarni R, Kumagai T, Lafon A, Lafton A, Latgé J-P, Li W, Lord A, et al. 2005. Genomic sequence of the pathogenic and allergenic filamentous fungus *Aspergillus fumigatus*. *Nature* 438:1151–1156. <http://dx.doi.org/10.1038/nature04332>.
 37. Suliman HS, Appling DR, Robertus JD. 2007. The gene for cobalamin-independent methionine synthase is essential in *Candida albicans*: a potential antifungal target. *Arch Biochem Biophys* 467:218–226. <http://dx.doi.org/10.1016/j.abb.2007.09.003>.
 38. Sienko M, Natorff R, Zieliński Z, Hejduk A, Paszewski A. 2007. Two *Aspergillus nidulans* genes encoding methylenetetrahydrofolate reductases are up-regulated by homocysteine. *Fungal Genet Biol* 44:691–700. <http://dx.doi.org/10.1016/j.fgb.2006.12.002>.
 39. Grynberg M, Topczewski J, Godzik A. 2000. The *Aspergillus nidulans* *cysA* gene encodes a novel type of serine O-acetyltransferase which is homologous to homoserine O-acetyltransferases. *Microbiology* 146:2695–2703.
 40. Perrin RM, Fedorova ND, Bok JW, Cramer RA, Wortman JR, Kim HS, Nierman WC, Keller NP. 2007. Transcriptional regulation of chemical diversity in *Aspergillus fumigatus* by LaeA. *PLoS Pathog* 3:e50. <http://dx.doi.org/10.1371/journal.ppat.0030050>.
 41. Wiemann P, Guo C, Palmer JM, Sekonyela R, Wang CCC. 2013. Prototype of an intertwined secondary-metabolite supercluster. *Proc Natl Acad Sci U S A* 110:17065–17070. <http://dx.doi.org/10.1073/pnas.1313258110>.
 42. Schoberle TJ, Nguyen-Coleman CK, Herold J, Yang A, Weirauch M, Hughes TR, McMurray JS, May GS. 2014. A novel C2H2 transcription factor that regulates *gliA* expression interdependently with GliZ in *Aspergillus fumigatus*. *PLoS Genet* 10:e1004336. <http://dx.doi.org/10.1371/journal.pgen.1004336>.
 43. Bok JW, Chung D, Balajee SA, Marr KA, Andes D, Nielsen KF, Frisvad JC, Kirby KA, Keller NP. 2006. GliZ, a transcriptional regulator of gliotoxin biosynthesis, contributes to *Aspergillus fumigatus* virulence. *Infect Immun* 74:6761–6768. <http://dx.doi.org/10.1128/IAI.00780-06>.
 44. Welch TR, Williams RM. 2014. Epidithiodioxopiperazines. Occurrence, synthesis and biogenesis. *Nat Prod Rep* 31:1376–1404. <http://dx.doi.org/10.1039/C3NP70097F>.
 45. Amatov T, Jahn U. 2014. Gliotoxin: nature’s way of making the epidithiol bridge. *Angew Chem Int Ed Engl* 53:3312–3314. <http://dx.doi.org/10.1002/anie.201310982>.
 46. Grillo MA, Colombatto S. 2008. S-Adenosylmethionine and its products. *Amino Acids* 34:187–193. <http://dx.doi.org/10.1007/s00726-007-0500-9>.
 47. Lin D-W, Chung BP, Kaiser P. 2014. S-Adenosylmethionine limitation induces p38 mitogen-activated protein kinase and triggers cell cycle arrest in G1. *J Cell Sci* 127:50–59. <http://dx.doi.org/10.1242/jcs.127811>.
 48. MacFarlane AJ, Liu X, Perry CA, Flodby P, Allen RH, Stabler SP, Stover PJ. 2008. Cytoplasmic serine hydroxymethyltransferase regulates the metabolic partitioning of methylenetetrahydrofolate but is not essential in mice. *J Biol Chem* 283:25846–25853. <http://dx.doi.org/10.1074/jbc.M802671200>.
 49. Piper MD, Hong SP, Ball GE, Dawes IW. 2000. Regulation of the balance of one-carbon metabolism in *Saccharomyces cerevisiae*. *J Biol Chem* 275:30987–30995. <http://dx.doi.org/10.1074/jbc.M004248200>.

50. Lessing F, Kniemeyer O, Wozniok I, Loeffler J, Kurzai O, Haertl A, Brakhage AA. 2007. The *Aspergillus fumigatus* transcriptional regulator AfYap1 represents the major regulator for defense against reactive oxygen intermediates but is dispensable for pathogenicity in an intranasal mouse infection model. *Eukaryot Cell* 6:2290–2302. <http://dx.doi.org/10.1128/EC.00267-07>.
51. Kacprzak MM, Lewandowska I, Matthews RG, Paszewski A. 2003. Transcriptional regulation of methionine synthase by homocysteine and choline in *Aspergillus nidulans*. *Biochem J* 376:517–524. <http://dx.doi.org/10.1042/BJ20030747>.
52. Martinez-Pastor B, Cosentino C, Mostoslavsky R. 2013. A tale of metabolites: the cross-talk between chromatin and energy metabolism. *Cancer Discov* 3:497–501. <http://dx.doi.org/10.1158/2159-8290.CD-13-0059>.
53. Dolan SK, O’Keeffe G, Jones GW, Doyle S. 2015. Resistance is not futile: gliotoxin biosynthesis, functionality and utility. *Trends Microbiol* 23: 419–428. <http://dx.doi.org/10.1016/j.tim.2015.02.005>.
54. Mabey Gilsean J, Cooley J, Bowyer P. 2012. CADRE: the Central *Aspergillus* Data REpository 2012. *Nucleic Acids Res* 40:D660–D666. <http://dx.doi.org/10.1093/nar/gkr971>.